AD-A142 478 AN EXPERIMENTAL INVESTIGATION OF THE IMPROVEMENT IN THE 1/1
RECEPTION OF TM (..(U) MEGAPULSE INC BEDFORD MASS
F M TINGLEY ET AL. MAY 84 RADC-TR-84-91
UNCLASSIFIED F19628-80-C-0148 F/G 17/2.1 NL

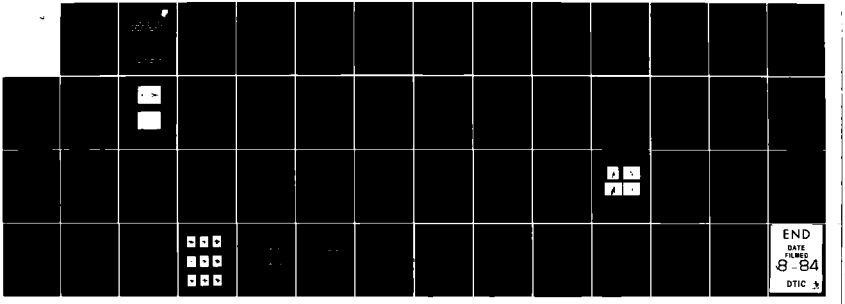

END
DATE FILMED
8-84
DTIC

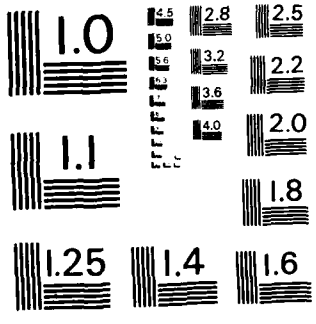

MICROCOPY RESOLUTION TEST CHART
NATIONAL BUREAU OF STANDARDS - 1963 - A

(12)

AD-A142 478

DTIC FILE COPY

RADC-TR-84-91
Interim Report
May 1984

AN EXPERIMENTAL INVESTIGATION OF THE IMPROVEMENT IN THE RECEPTION OF TM-POLARIZED LF WAVES WITH A TWO-ELEMENT SPACED ARRAY

Megapulse, Inc.

Frederick M. Tingley
Royce C. Kahler

ROME AIR DEVELOPMENT CENTER
Air Force Systems Command
Griffiss Air Force Base, NY 13441

This report has been reviewed by the RADC Public Affairs Office (PA) and is releasable to the National Technical Information Service (NTIS). At NTIS it will be releasable to the general public, including foreign nations.

RADC-TR-84-91 has been reviewed and is approved for publication.

APPROVED: Wayne I. Klemetti

WAYNE I. KLEMETTI
Project Engineer

APPROVED: Allan C. Schell

ALLAN C. SCHELL
Chief, Electromagnetic Sciences Division

FOR THE COMMANDER: John A. Ritz

JOHN A. RITZ
Acting Chief, Plans Office

If your address has changed or if you wish to be removed from the RADC mailing list, or if the addressee is no longer employed by your organization, please notify RADC (EEPS) Hanscom AFB MA 01731. This will assist us in maintaining a current mailing list.

Do not return copies of this report unless contractual obligations or notices on a specific document requires that it be returned.

UNCLASSIFIED

SECURITY CLASSIFICATION OF THIS PAGE

REPORT DOCUMENTATION PAGE

1a. REPORT SECURITY CLASSIFICATION UNCLASSIFIED	1b. RESTRICTIVE MARKINGS N/A
2a. SECURITY CLASSIFICATION AUTHORITY N/A	3. DISTRIBUTION/AVAILABILITY OF REPORT Approved for public release; distribution unlimited
2b. DECLASSIFICATION/DOWNGRADING SCHEDULE N/A	
4. PERFORMING ORGANIZATION REPORT NUMBER(S) None	5. MONITORING ORGANIZATION REPORT NUMBER(S) RADC-TR-84-91
6a. NAME OF PERFORMING ORGANIZATION Megapulse, Inc. 6b. OFFICE SYMBOL (If applicable) N/A	7a. NAME OF MONITORING ORGANIZATION Rome Air Development Center (EEPS)
6c. ADDRESS (City, State and ZIP Code) 8 Preston Court Bedford MA 01730	7b. ADDRESS (City, State and ZIP Code) Hanscom AFB MA 01731
8a. NAME OF FUNDING/SPONSORING ORGANIZATION Rome Air Development Center 8b. OFFICE SYMBOL (If applicable) EEPS	9. PROCUREMENT INSTRUMENT IDENTIFICATION NUMBER F19628-80-C-0146
8c. ADDRESS (City, State and ZIP Code) Hanscom AFB MA 01731	10. SOURCE OF FUNDING NOS. PROGRAM ELEMENT NO.: 62702F PROJECT NO.: 4600 TASK NO.: 16 WORK UNIT NO.: 44
11. TITLE (Include Security Classification) An Experimental Investigation of the	
12. PERSONAL AUTHOR(S) Frederick M. Tingley, Royce C. Kahler	
13a. TYPE OF REPORT Interim 13b. TIME COVERED FROM _____ TO _____	14. DATE OF REPORT (Yr., Mo., Day) May 1984 15. PAGE COUNT
16. SUPPLEMENTARY NOTATION None	

17. COSATI CODES			18. SUBJECT TERMS (Continue on reverse if necessary and identify by block number)
FIELD	GROUP	SUB. GR.	Two-element phased array; Radio waves; Transverse Magnetic; Signal-to-noise ratios; Low-frequency
17	02		
20	14		

19. ABSTRACT (Continue on reverse if necessary and identify by block number)

For this study, a 2-element spaced array antenna system was developed and tested. This array consisted of two well-spaced vertical loops combined with a microwave link. The array was tested to show improvements in signal-to-noise ratio over omnidirectional antennas, using received transmissions from an aircraft towing a long wire antenna. Gains in signal-to-noise ratio of up to 12.8 dB were demonstrated.

20. DISTRIBUTION/AVAILABILITY OF ABSTRACT UNCLASSIFIED/UNLIMITED ☒ SAME AS RPT. ☐ DTIC USERS ☐	21. ABSTRACT SECURITY CLASSIFICATION UNCLASSIFIED
22a. NAME OF RESPONSIBLE INDIVIDUAL Wayne I. Klemetti	22b. TELEPHONE NUMBER (Include Area Code) 617-861-4239 22c. OFFICE SYMBOL RADC (EEPS)

DD FORM 1473, 83 APR EDITION OF 1 JAN 73 IS OBSOLETE.

UNCLASSIFIED

SECURITY CLASSIFICATION OF THIS PAGE

Block 11 (Title) Cont'd

Improvement in the Reception of TM-Polarized LF Waves with a Two-element Spaced Array

TABLE OF CONTENTS

TABLE OF CONTENTS
(continued)

LIST OF ILLUSTRATIONS

TABLE OF CONTENTS
(continued)

LIST OF ILLUSTRATIONS

ABSTRACT

A two-element spaced array system for reception of low frequency transverse magnetic radio waves was studied, constructed, and tested. It consisted of two well-spaced vertical loops combined through a microwave link and an adjustable delay. It was tested against atmospheric noise on transmissions from an aircraft towing a long wire antenna. Improvements of up to 12.8 dB in signal-to-noise ratio over omnidirectional antennas were demonstrated.

Acknowledgements

The authors gratefully acknowledge the help and assistance of the many people who made this program possible. RADC personnel were especially helpful; Mr. John L. Heckscher helped with his technical support and Messrs. Wayne I. Klemetti, John P. Turtle and Robert P. Pagliarulo provided valuable logistic support.

We thank Mr. Kenneth Glover of the Weather Radar Facility of the U.S. Air Force and his personnel at Sudbury for the use of their facilities and their assistance.

We also thank Mr. Anthony Costa, Chief of Fire Control of the State Fire Marshall's office, for the use of the fire tower on Oak Ridge in Harvard, MA. Also, if it had not been for the permission given by Mr. Manuel Ferjulian of Standard Orchard in Hudson, MA to set our remote site on Gospel Hill, it is doubtful that we would have obtained positive results as easily. The authors are also in great debt to Mr. Robert Harrison for the loan of personal equipment, and Mr. James Donohoe for his experimental expertise and help in the field. Dr. E.A. Lewis participated in an advisory capacity in formulating the basic concepts of the work and contributing Appendix A.

1. INTRODUCTION AND BACKGROUND

In 1980, it was suggested that an array of simple low-frequency antennas might improve the signal-to-noise ratio (SNR) beyond that obtainable with the simple loop. More detailed calculations* showed that with a certain antenna spacing there should be an improvement in signal-to-noise ratio even if the noise were distributed uniformly around the horizon. A more likely scenario would postulate noise from more or less discrete directions. Noise from one azimuth could be suppressed by orienting the antenna loops, while noise from another could be suppressed by properly phasing the array. Sometimes it might even be possible to reduce the noise of a third storm direction by judiciously choosing the combination of parameters. In the two-storm case a much greater improvement in SNR was expected than with uniformly distributed noise, providing, of course, that the wanted signal came from a different direction than the noise. This report describes an experimental study of some of these concepts.

In order to assess the noise environment for purposes of maximizing the SNR, it was important to know the main direction of arrival of the sferics noise. Accordingly, a direction finder and two-loop spaced array system was assembled and its capabilities demonstrated; improvements of over 12 dB in the received signal-to-noise ratio from an in-flight aircraft towing a long antenna were shown. The direction finder (Watson-Watt type) displayed on an oscilloscope radial traces in directions corresponding to the azimuth of the noise sources, with radial lengths proportional to the amplitudes of the received pulses.

---

*Lewis & Heckscher memo "Potential Improvement in the Reception of TM and TE Polarized LF Waves with Two and Three Spaced Antennas on the Ground"

The array consisted of two loop antennas separated by about four kilometers but connected by a telemetry link. By inserting a variable delay between the two received signals, summing, filtering and detecting, the signals were caused to add and the noise was caused to cancel. Also, the loop antennas were manually turned so as to optimally position their nulls for greater noise reduction.

2. THE NOISE

The dominant source of noise at low and very low radio frequencies is lightning discharges. The currents flowing in the strokes from cloud to cloud or from earth to cloud produce large radiated fields with spectral density that shown in Figure 2.1. Various aspects of this noise - the field as a function of distance, the spectra of the average noise from many distant storms, and the amplitude distribution of the band limited noise envelope - are shown in Figures 2.2 through 2.4. At the lower amplitudes, this envelope follows a Rayleigh distribution implying that the function itself is Gaussian. Electrical discharges commonly occur in individual storm cells belonging to weather fronts and moving across the earth's surface. Each cell becomes active independently, remains active for awhile, and dies. Meanwhile, a new cell is born at some other position. The location of the source of noise and its direction and intensity as seen from the array changes with time. The changes are especially marked with local storms but also occur with storms over a thousand miles distant.

The noise of greatest amplitude as measured in the northeastern United States originates in local storms, generally in late Spring, Summer, and early Fall afternoons. At all seasons, but predominantly in the afternoon, storms in the southeastern United States provide a medium range of amplitudes. All of this is added to a more or less continuous background noise originating in storms throughout the world, especially in South America, Africa, and Indonesia.

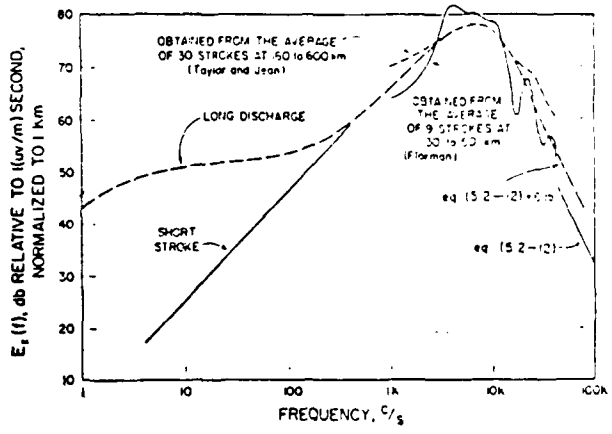

Fig.2.1 Calculated and observed frequency spectrum of the radiation component of field strength from an average cloud to ground discharge, normalized to a distance of 1 km (precursor fields have been neglected).

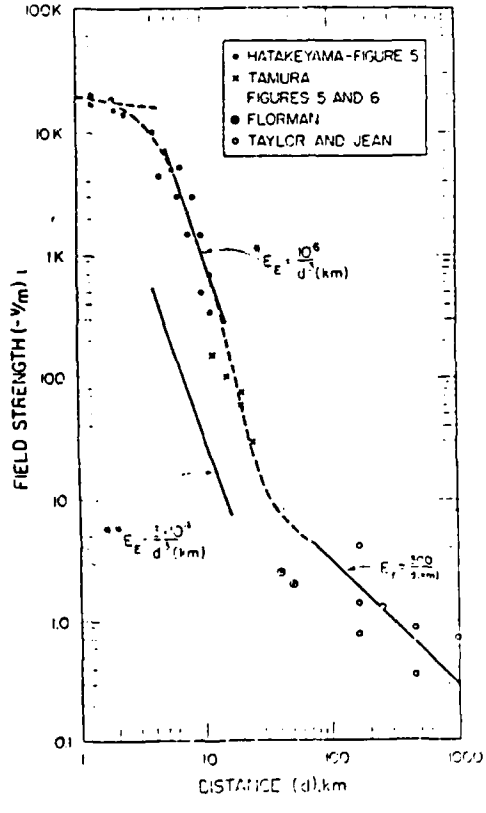

Figure 2.2 Peak electric field variation from lightning discharges.

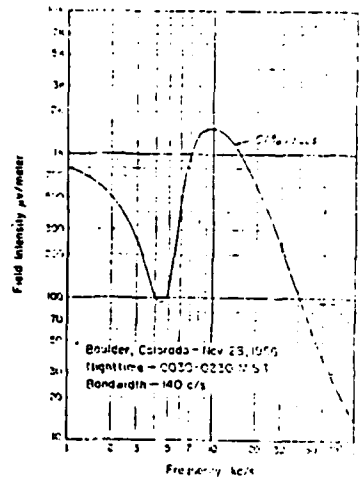

Fig.2.3 Measured frequency spectra of atmospheric noise envelope

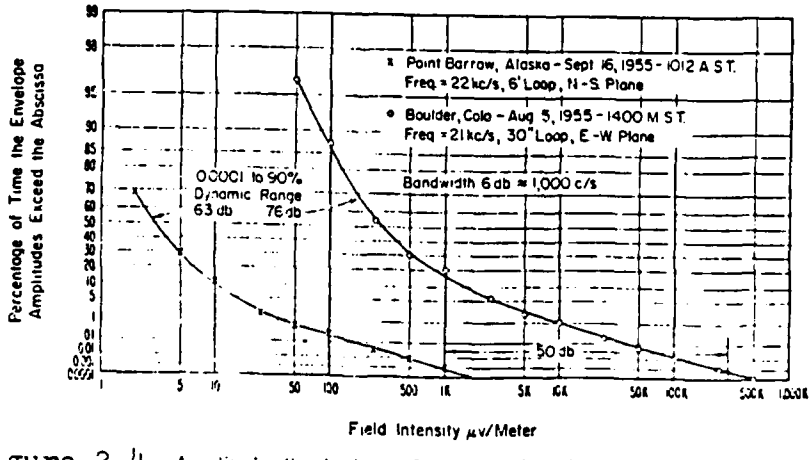

Figure 2.4. Amplitude distributions of atmospheric noise envelopes showing maximum range of amplitude level observed at all five stations.

(all from Watt, "VLF Radio Engineering")

3. THE ANTENNA

The antennas used in this study were loops oriented for transverse-magnetic polarization. Two loop antennas were separated by a distance s and positioned vertically, with axes horizontal and parallel. The signal from one (slave) loop was telemetered to the master station and added to the delayable signal from the other (master) loop. The amount of delay inserted determined the angle of the lobes and nulls, and changed the shape of the patterns. Each loop was manually rotatable so that the operators could aim or null the loop pattern in any azimuth, thus giving the antenna a second controllable parameter for the shaping of the pattern. The loop axes were always aligned and parallel to insure proper combinations.

The equation describing the array pattern (amplitude V versus azimuth θ) normalized to the response perpendicular to the line joining the two loops, is

$$V(\theta) = \sqrt{\frac{1 + \cos (ks \sin \theta - \phi)}{1 + \cos \phi}} \cos (\theta - \zeta) \qquad 3.1$$

where the gain of both loop channels is identical, k is the wave number ($= 360/\lambda$), ϕ is the delay in degrees ($= 360\tau f$), ζ is the direction in which the loop maximum is pointed, f is the frequency and τ is the time delay. This equation was originally derived for continuous wave signals, but can be used to null impulsive noise in narrow frequency bands. The narrow band component of a broadband impulsive waveform has a smoothly varying envelope, which rises to a peak and then decreases at rates determined by the bandwidth. The output of an actual narrow-band filter, such as a receiver I.F. strip, typically looks like that shown in Figure 3.1, and is commonly referred to as the filter "ringing". If two slowly decaying wave shapes, identical except that one is delayed 180 degrees with respect to the other, are summed, the result will be nearly complete

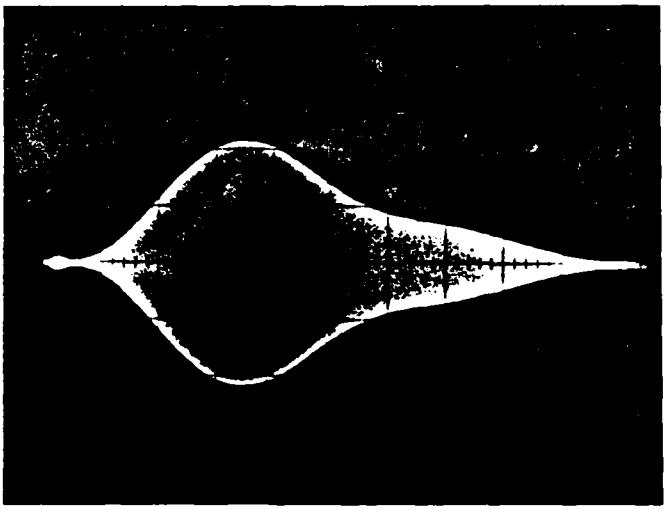

a. Bandwidth = 100 Hz

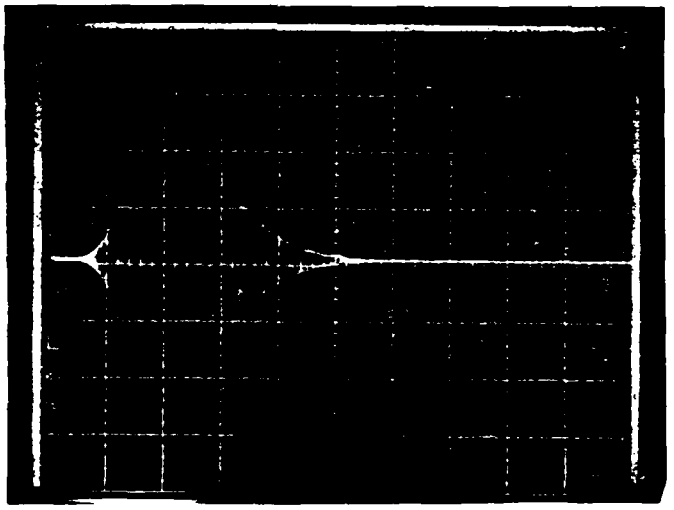

b. Bandwidth = 1000 Kz

Figure 3.1 Filter Ringing, Singer NM-12

cancellation. Equation 3.1 has been evaluated for a great variety of parameters. Figures 3.2 through 3.7 are a sampling of the resultant patterns. These represent the array only, the cosine term describing the effect of the loops has not been included.

For an illustration of how this array worked, assume that two loops have been placed on an east-west line, separated by a distance s, as shown in Figure 3.8. Suppose, also, that the desired signal is coming from the south and that sferics noise is arriving from a storm at azimuth θ. There are two basic ways in which the signals and noise arriving at the two loops can be processed for constructive or destructive addition: inversion (multiplication by -1) and 180° time delay. In the first case the signal or noise impulse arriving perpendicular to the baseline (south or north in the figure) will be cancelled over a wide frequency range by the addition of the inverted pulse from one loop to the unchanged pulse from the other. This is illustrated in Figure 3.9a. Impulses arriving from the east or west, inverted at one station and summed, will produce a positive going pulse followed by a negative going one (or vice versa), the time separation being the travel time from one station to the other. This will produce no wide band gain, but if the signals are bandpass filtered at a frequency for which the separation is about a half wavelength, the frequency components within the filter bandpass of the inverted and non-inverted pulses will combine constructively. An artificially introduced delay or a larger separation will change the angles and perhaps the number of maxima and nulls, but the effect is the same. The disadvantage of the inverting array is that the desired signal which is to be maximized is combined with a 180° lag, which is all right if it is CW but will cause distortion if it is modulated.

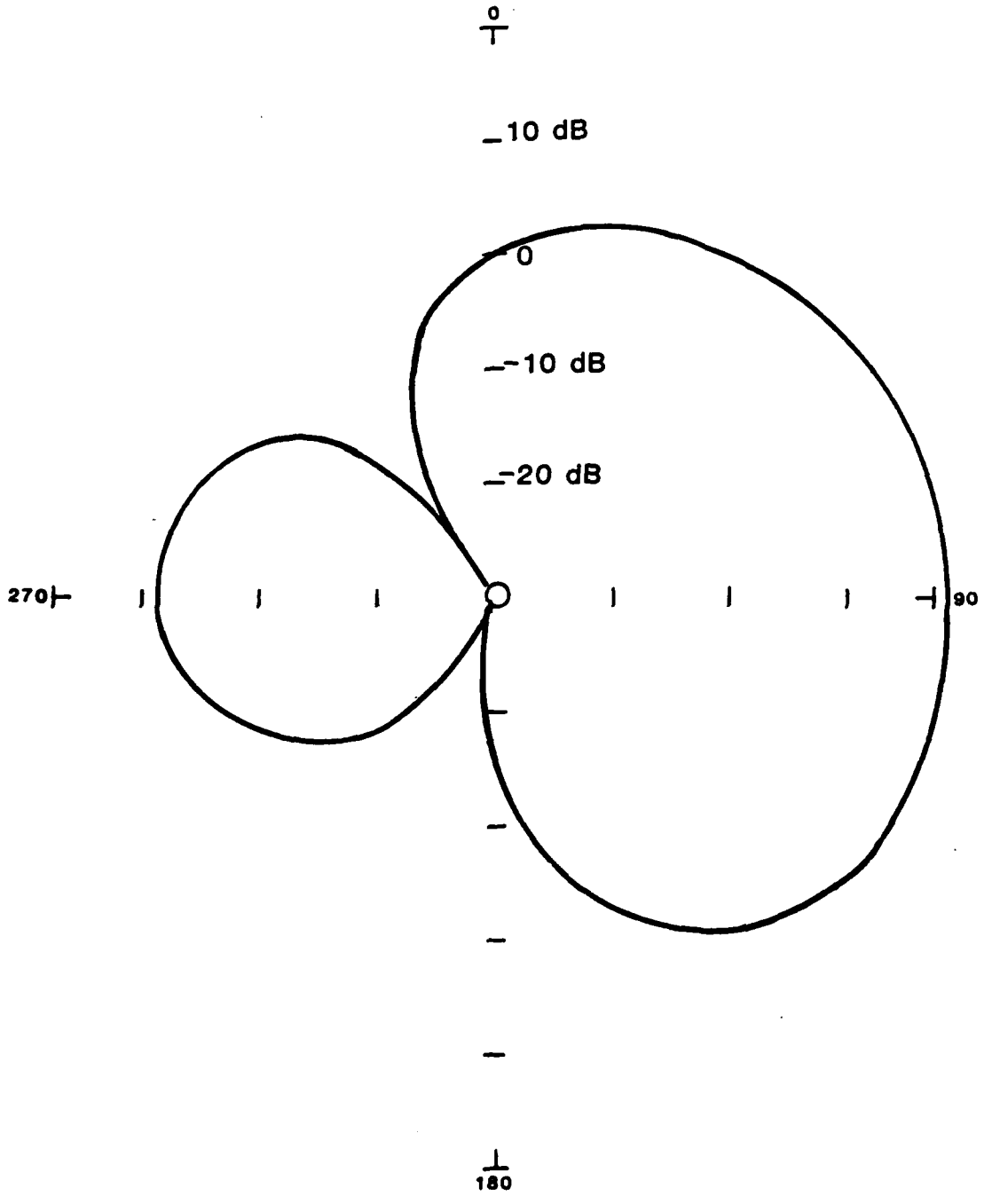

Figure 3.2
Array Pattern, ks=3.6°, ϕ=178°, rho=1

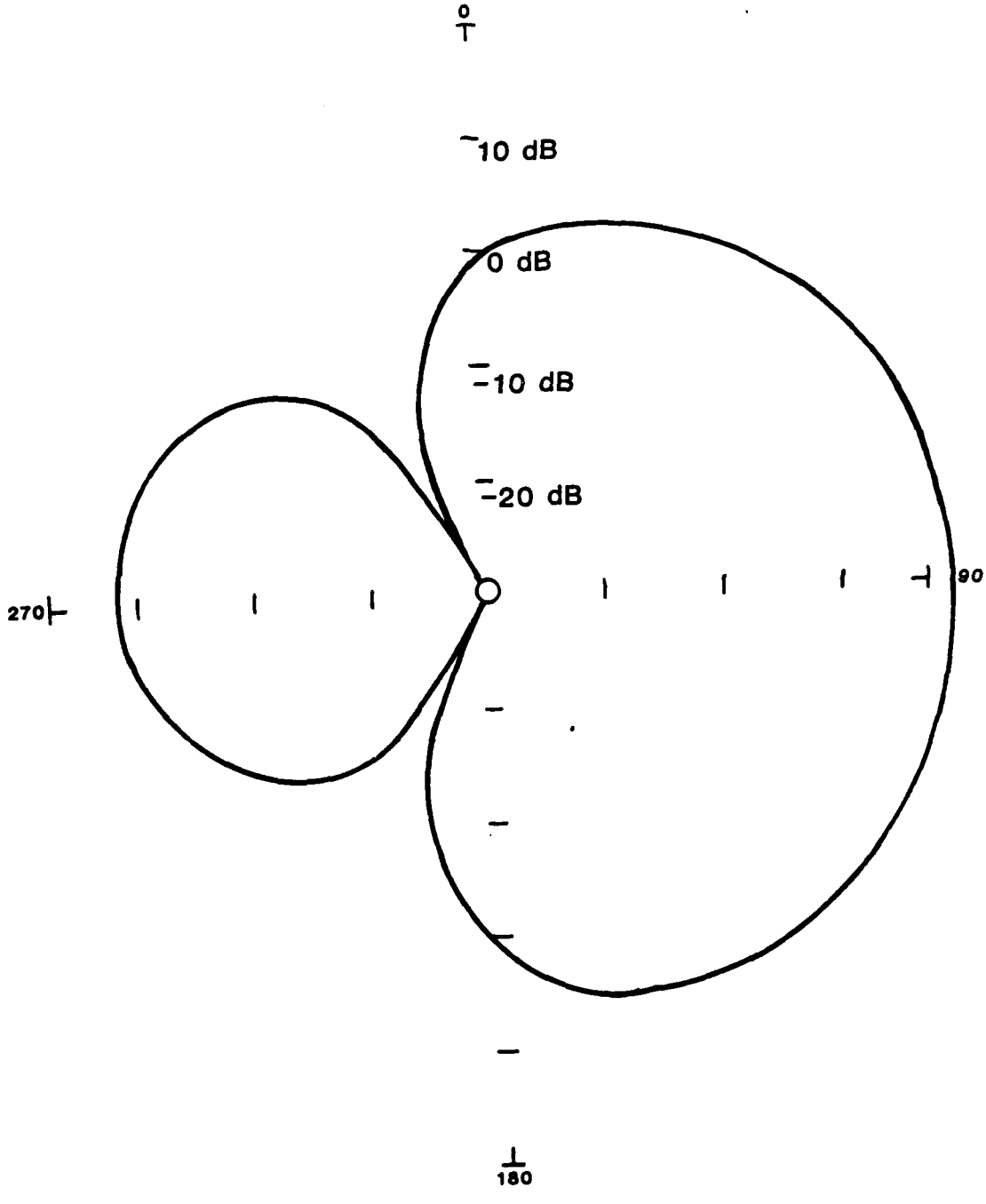

Figure 3.3
Array Pattern For ks=22.5°, ‡=170°, rho=1

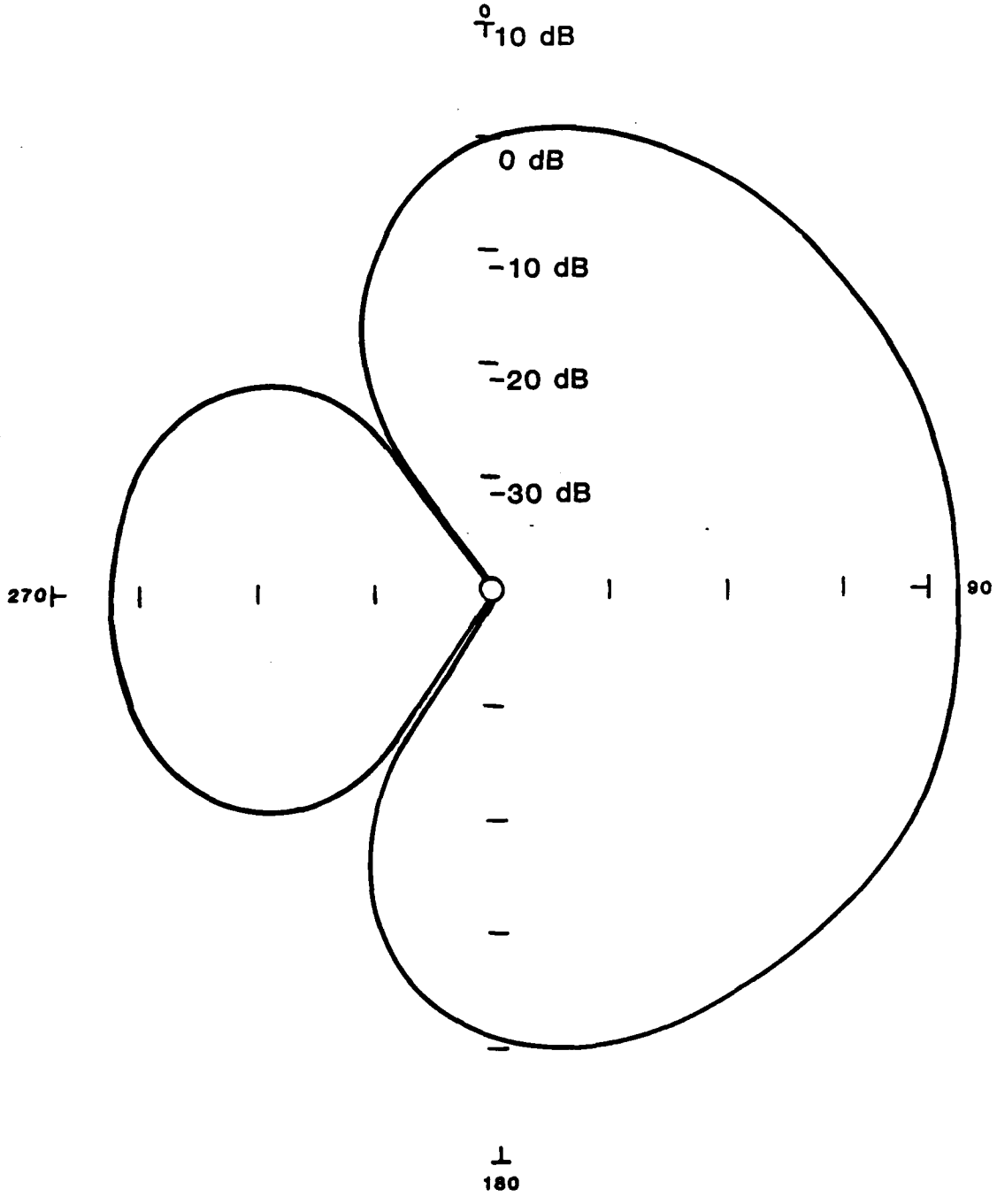

Figure 3.4
Array Pattern, ks=180°, ϕ=30°, rho=1

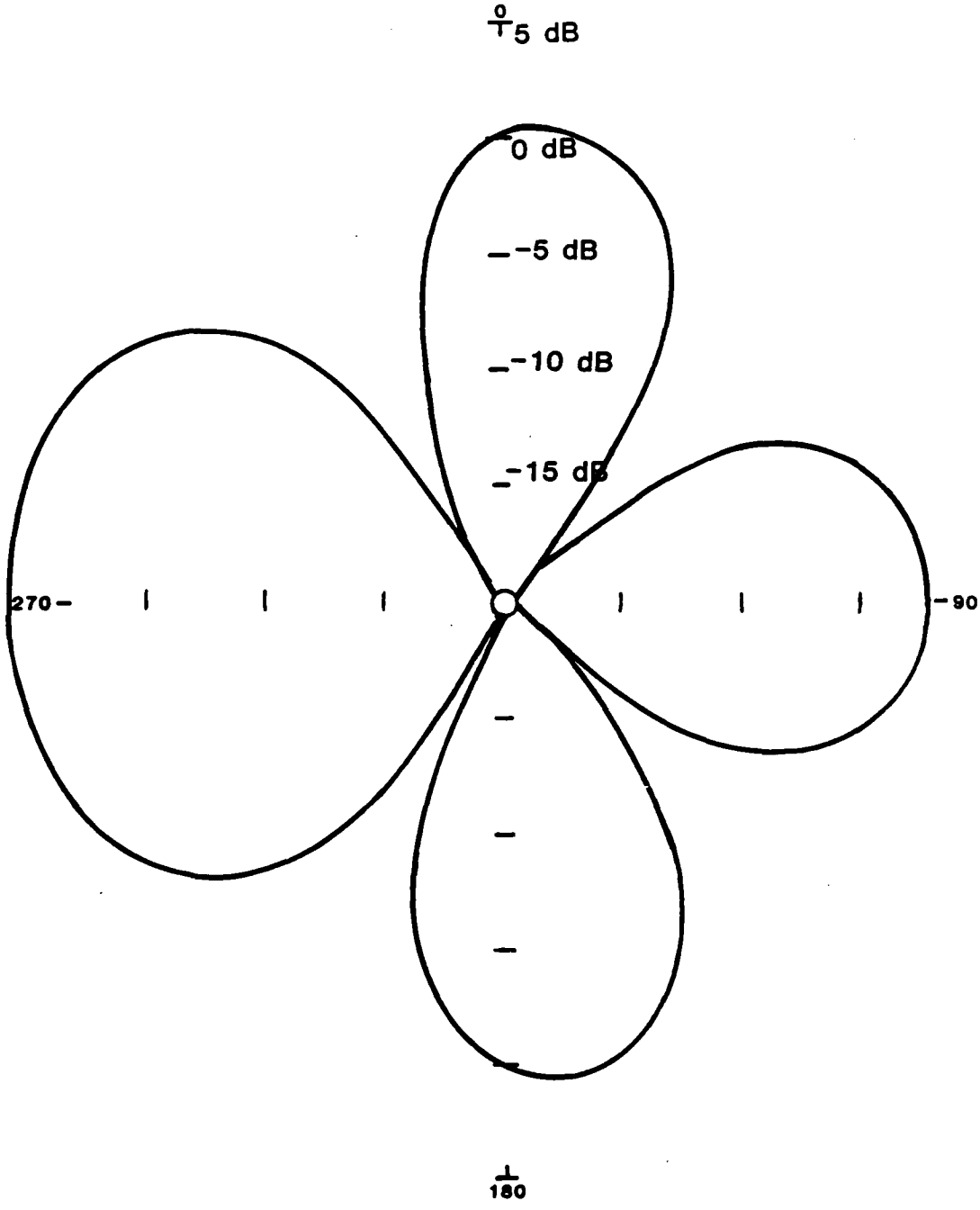

Figure 3.5
Array Pattern, ks=315°, ϕ=40°, rho=1

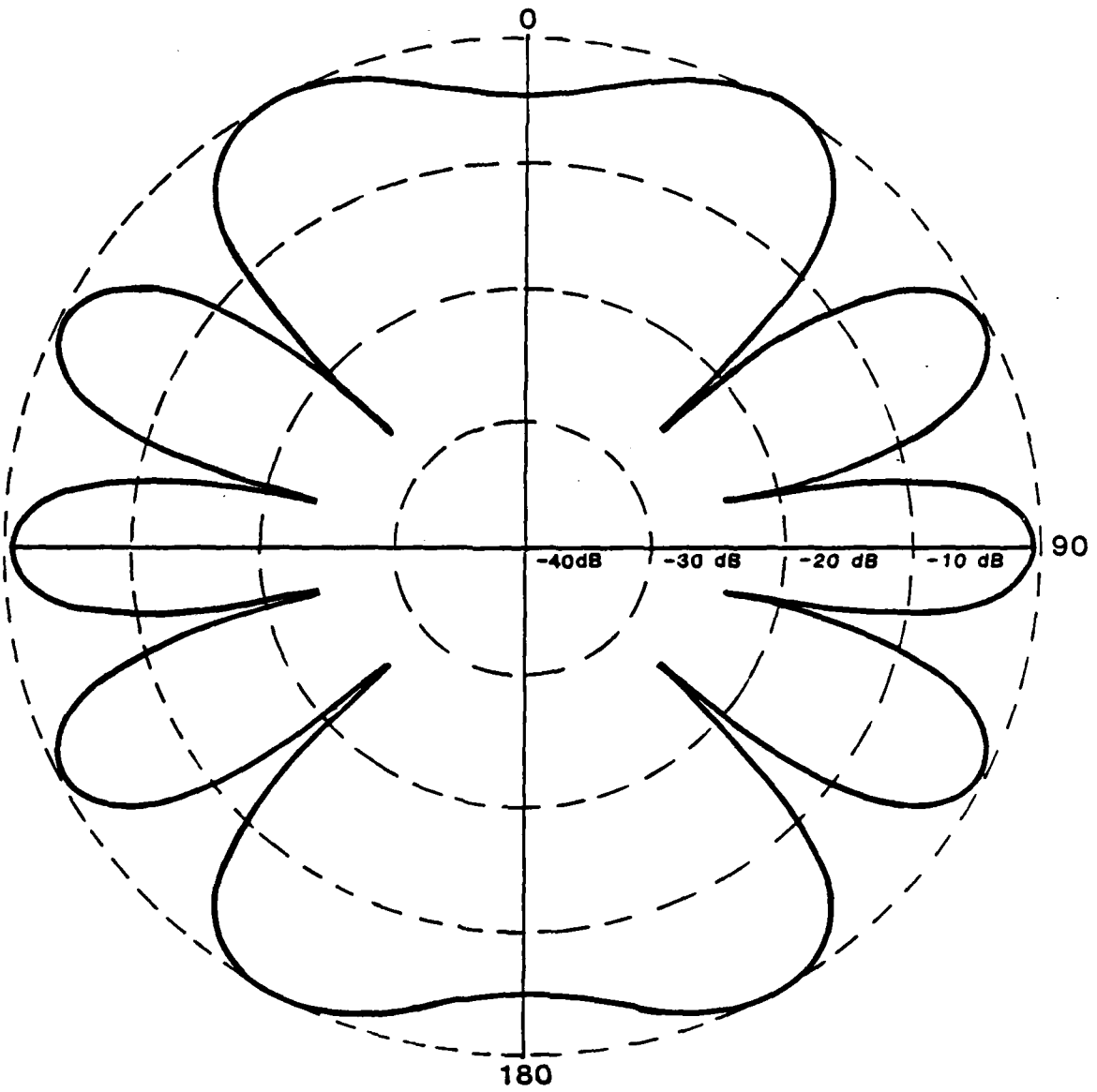

Figure 3.6

Array Pattern For ks=416°, ϕ=0°, rho=1

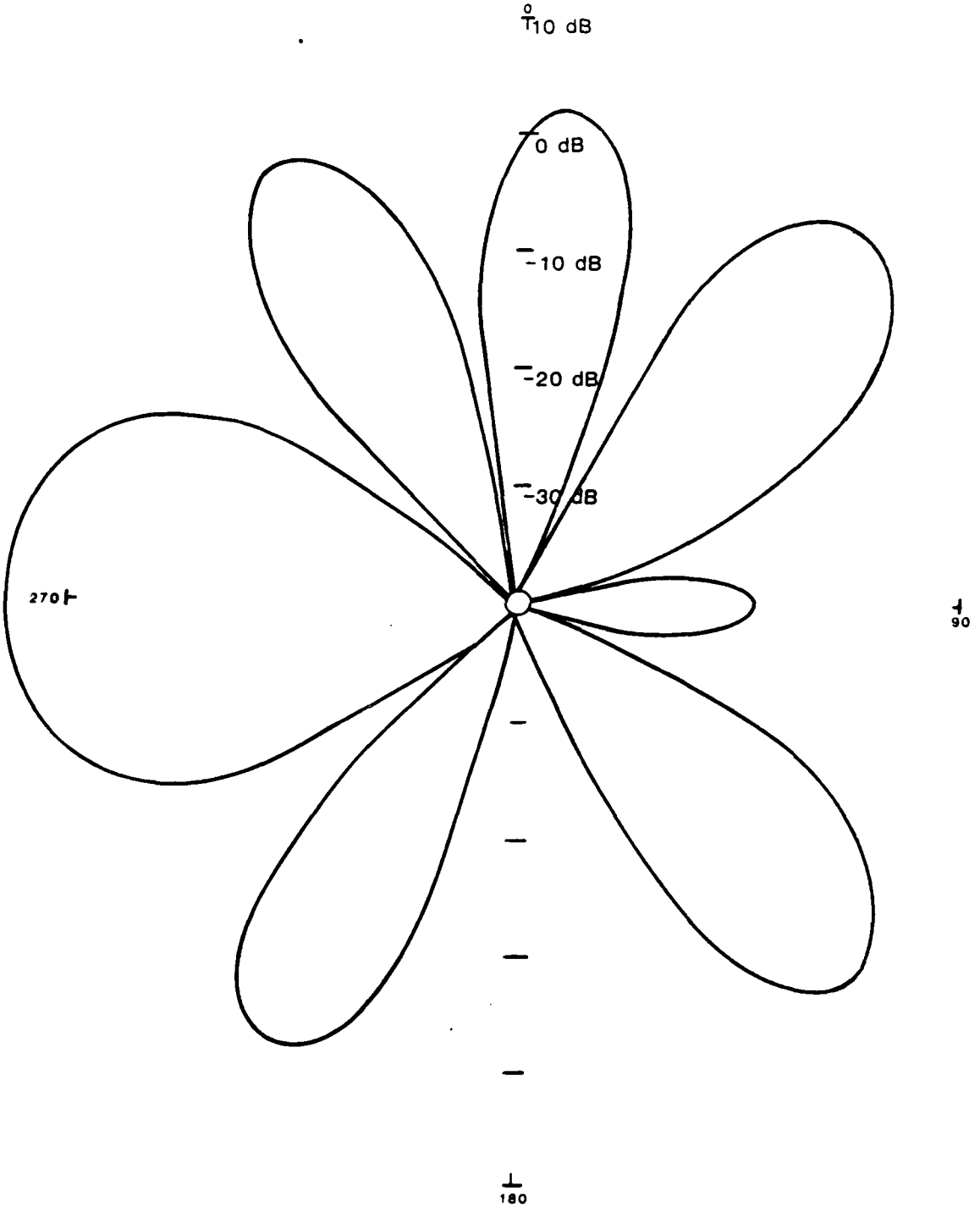

Figure 3.7
Array Pattern, ks=630°, ϕ=60°, rho=1

It seems preferable to combine in a manner that does not degrade the signal, but does the noise. If there are no artificial inversions introduced into the array depicted in Figure 3.8, signals arriving from the north or the south will be constructively added over a wide frequency band because they arrive at both loops at the same time as sketched in Figure 3.9. An impulse coming from the east will arrive at the western loop about half a period after it arrived at the eastern loop and, after summing and filtering, partly cancels itself. The cancellation is only partial because, unless the filtered bandwidth is zero, the amplitude will decay slightly in a half cycle.

If the Q of the filter is large, this error becomes negligible. For an information bandwidth of 100 Hz at 40 kHz, Q = 400. When it is desired to null noise from direction θ, the peak of the frequency component of interest of a noise pulse reaches the west station a time τ before the valley reaches the east station. To null this noise, delay the western pulse and add it to the eastern pulse. From the diagram

$$\tau c = \lambda/2 - s \sin\theta. \qquad 3.2$$

Expressing the delay as a fraction of the period in degrees,

$$\begin{aligned} 360\tau f &= 180 - 360(s/\lambda)\sin\theta \\ &= 180 - ks \sin\theta \qquad 3.3 \\ &= -\phi \end{aligned}$$

where c is the free space speed of light and ϕ is the delay in degrees used in Equation 3.1. If the western site is the slave, its signal is always delayed by the "teledelay", the sum of the propagation time from W to E and an equipment delay.

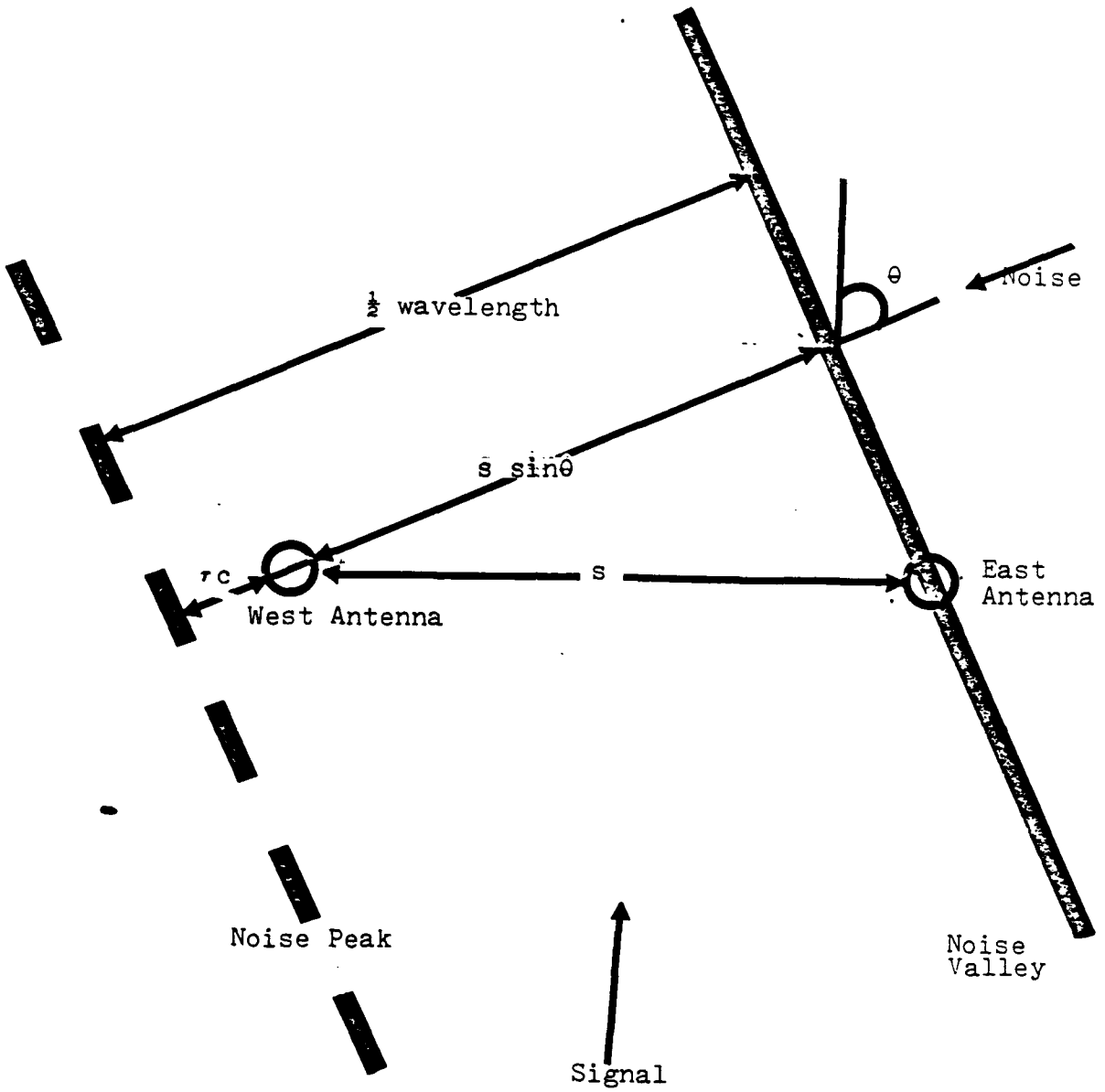

Figure 3.8 Array Geographics

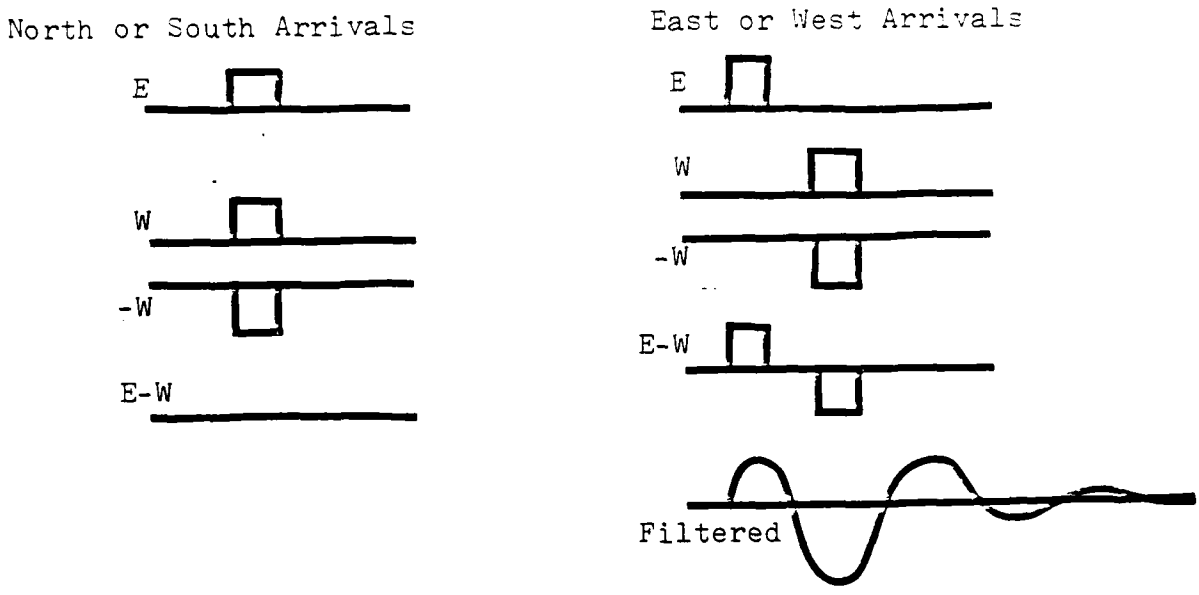

a. Inverted Array

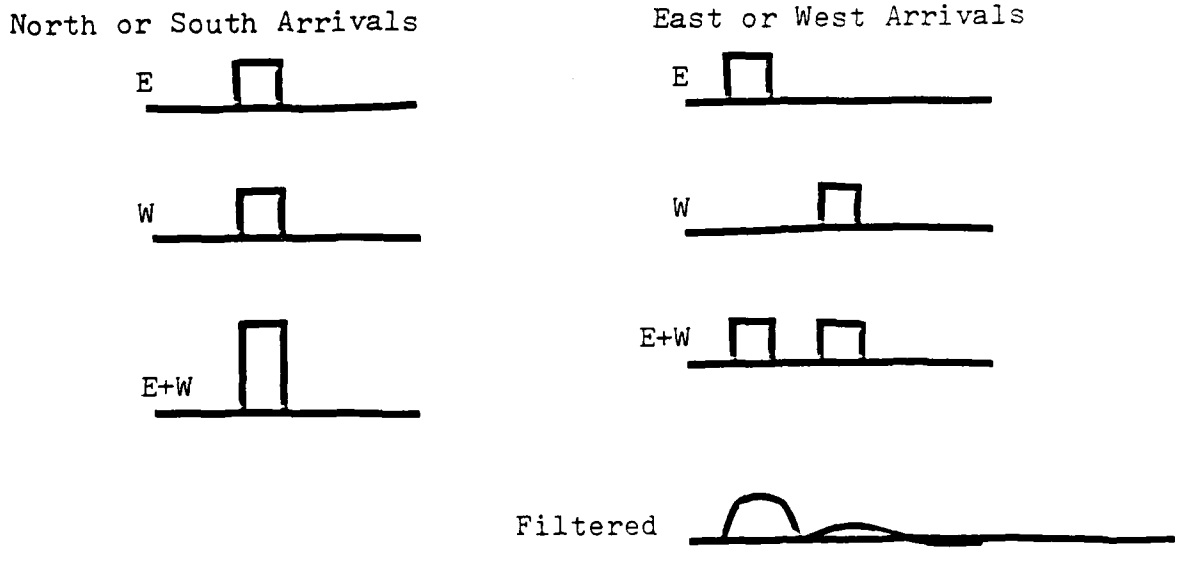

b. Non-Inverted Array

Figure 3.9 Array Pulse Addition

The delay to be inserted in the eastern channel is then the sum of the teledelay and the steering delay,

$$\Delta = \text{teledelay} - \phi/(.36f) \qquad 0 \leq \phi \leq 180 \text{ (f in kHz)} \qquad 3.4$$

$$= \text{teledelay} - \phi/(.36f) + 100/f \qquad 180 \leq \phi \leq 360$$

To better understand the action of the array, and as an aid in determining how best to steer it, the array equation was solved for the null angles for different delays. Some of the data is in Figures 3.10 through 3.12. If a lobe is not aimed directly at the source, a frequency modulation of the carrier will cause a change in the array pattern for the instantaneous frequency, and produce an amplitude modulation, which might distort the signal. The magnitude of this effect, for one case, is plotted in Figure 3.13. To help determine the array size, the width of the lobes and nulls is a major consideration. Figures 3.14 and 3.15 show these effects.

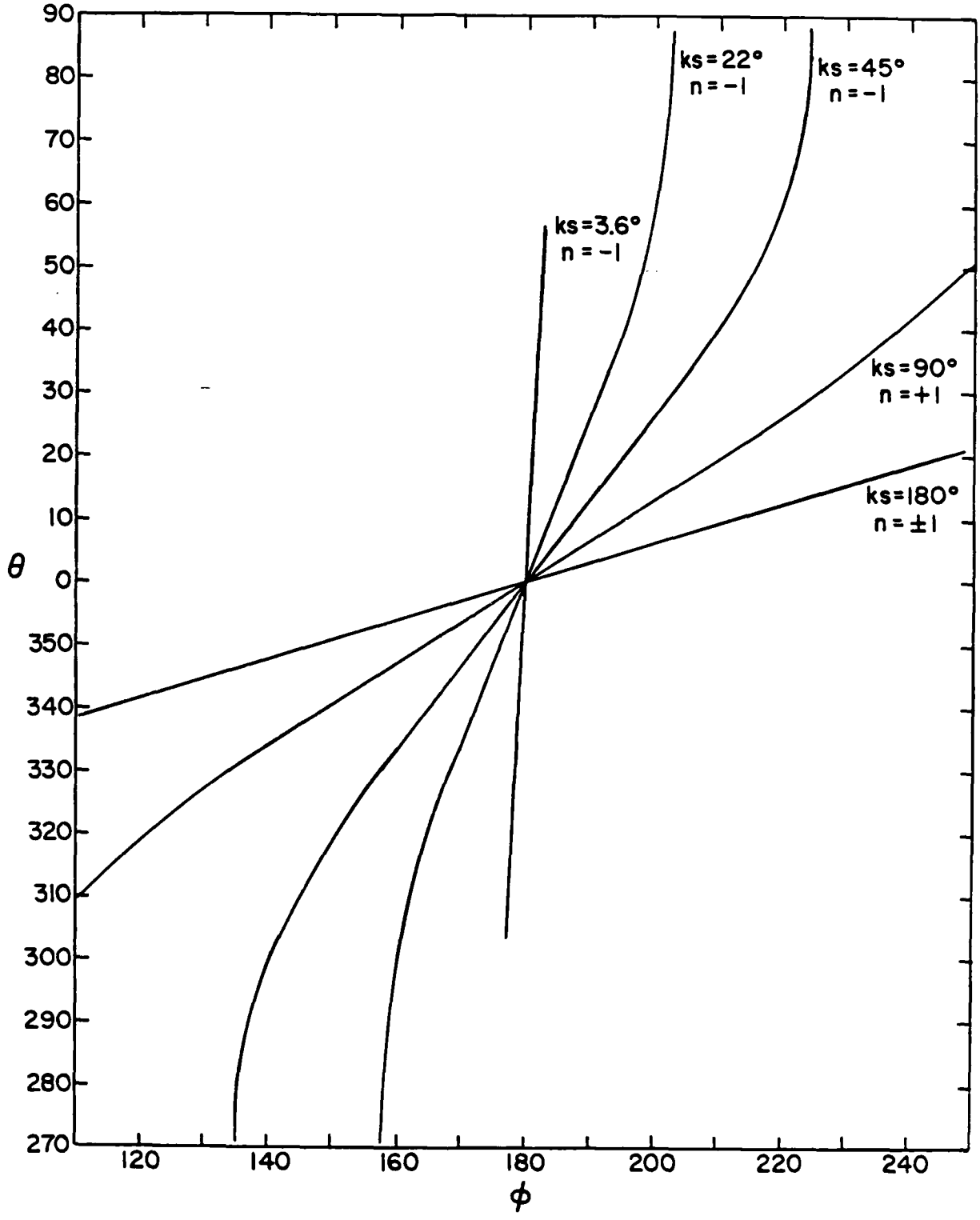

Figure 3.10

Array Nulls, Small Arrays

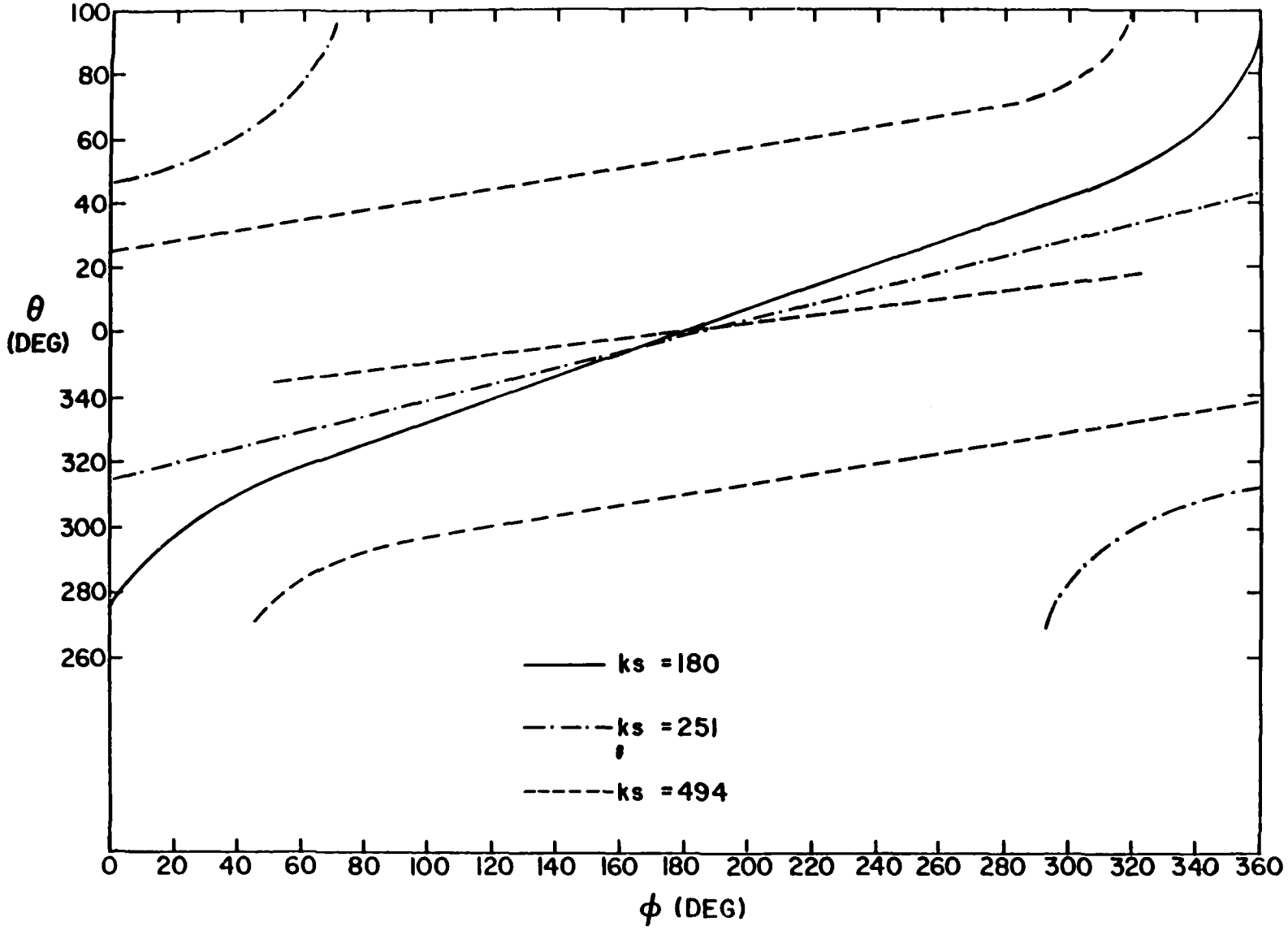

Figure 3.11

Array Null, Large Arrays

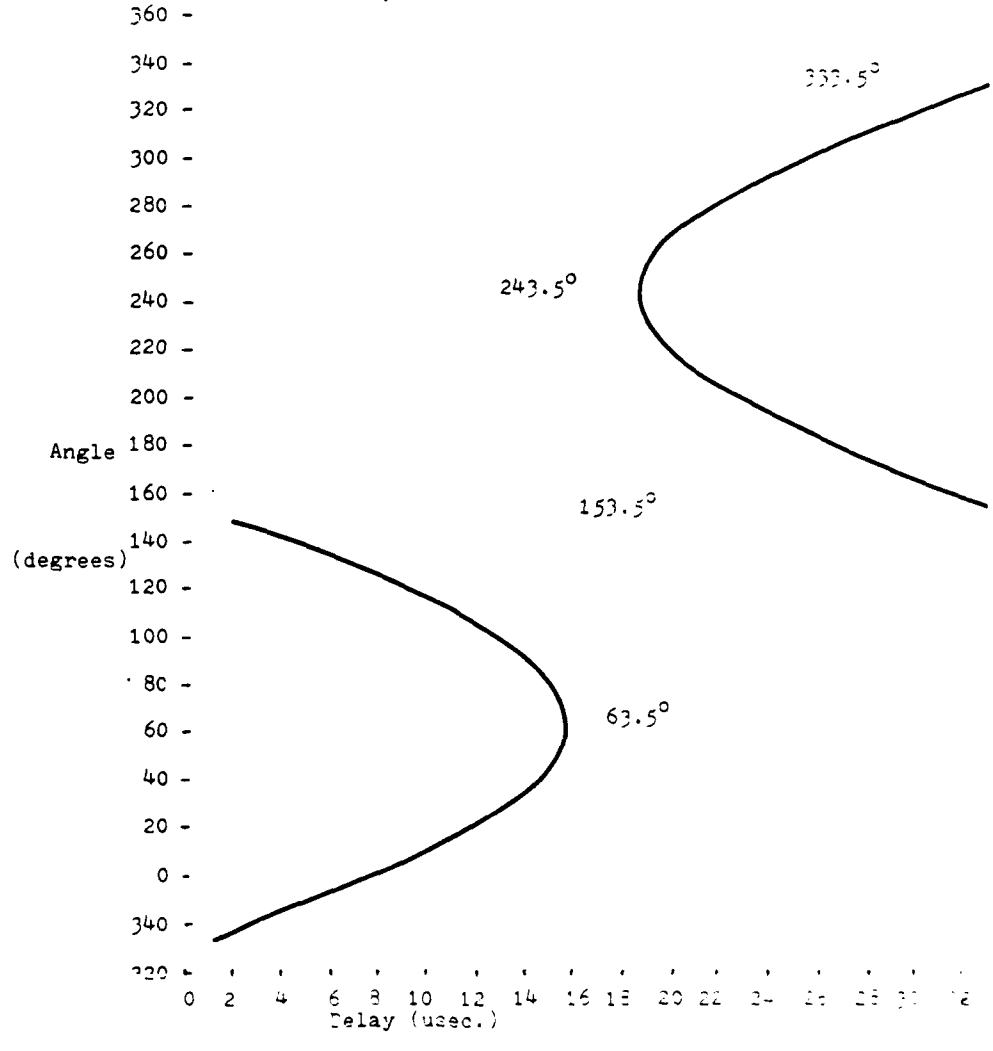

Figure 3.12 Null Angle versus Delay Time, [illegible] Hill Link (31 MHz)

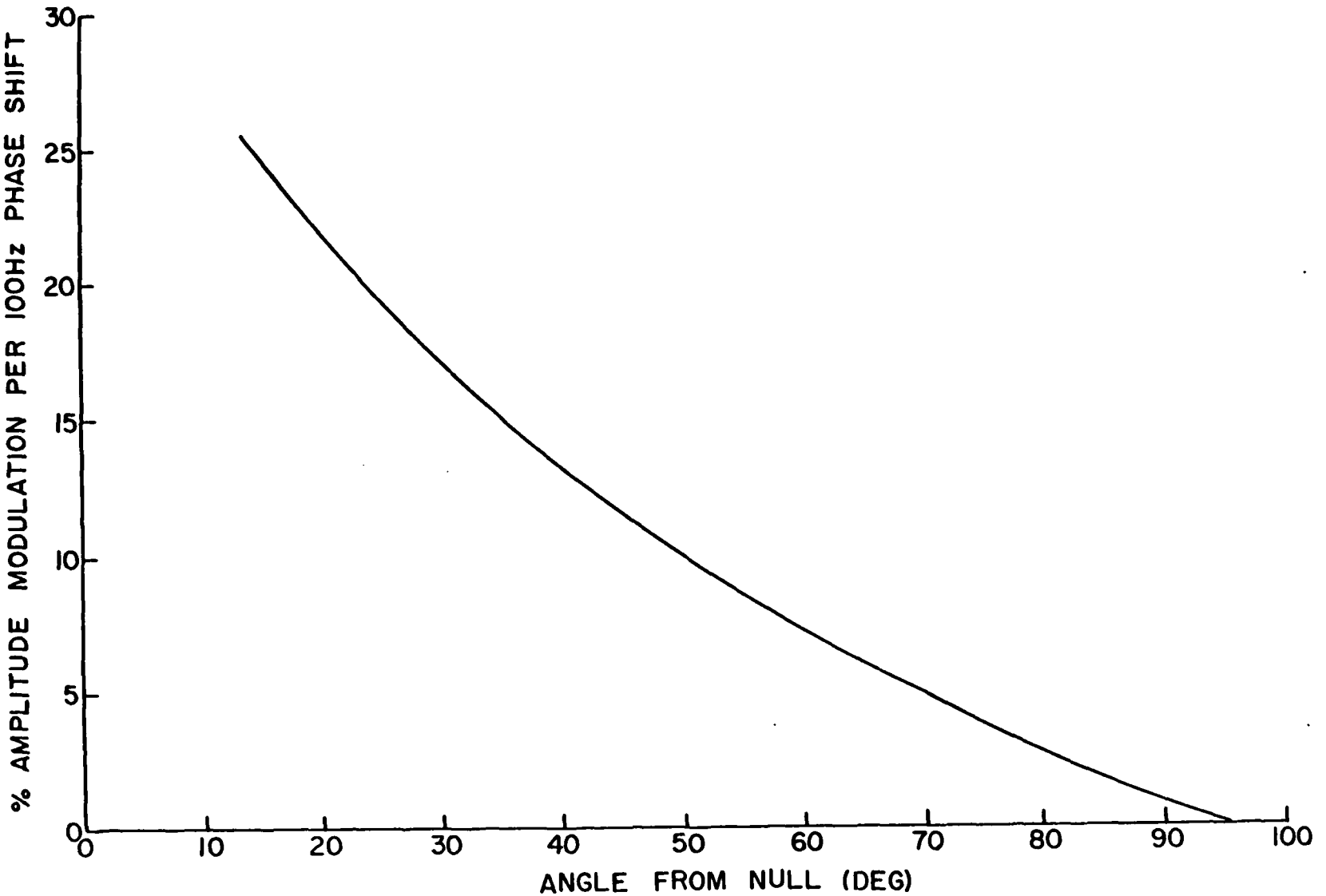

Figure 3.13

Amplitude Modulation Resulting from Antenna Pattern Changes with Frequency

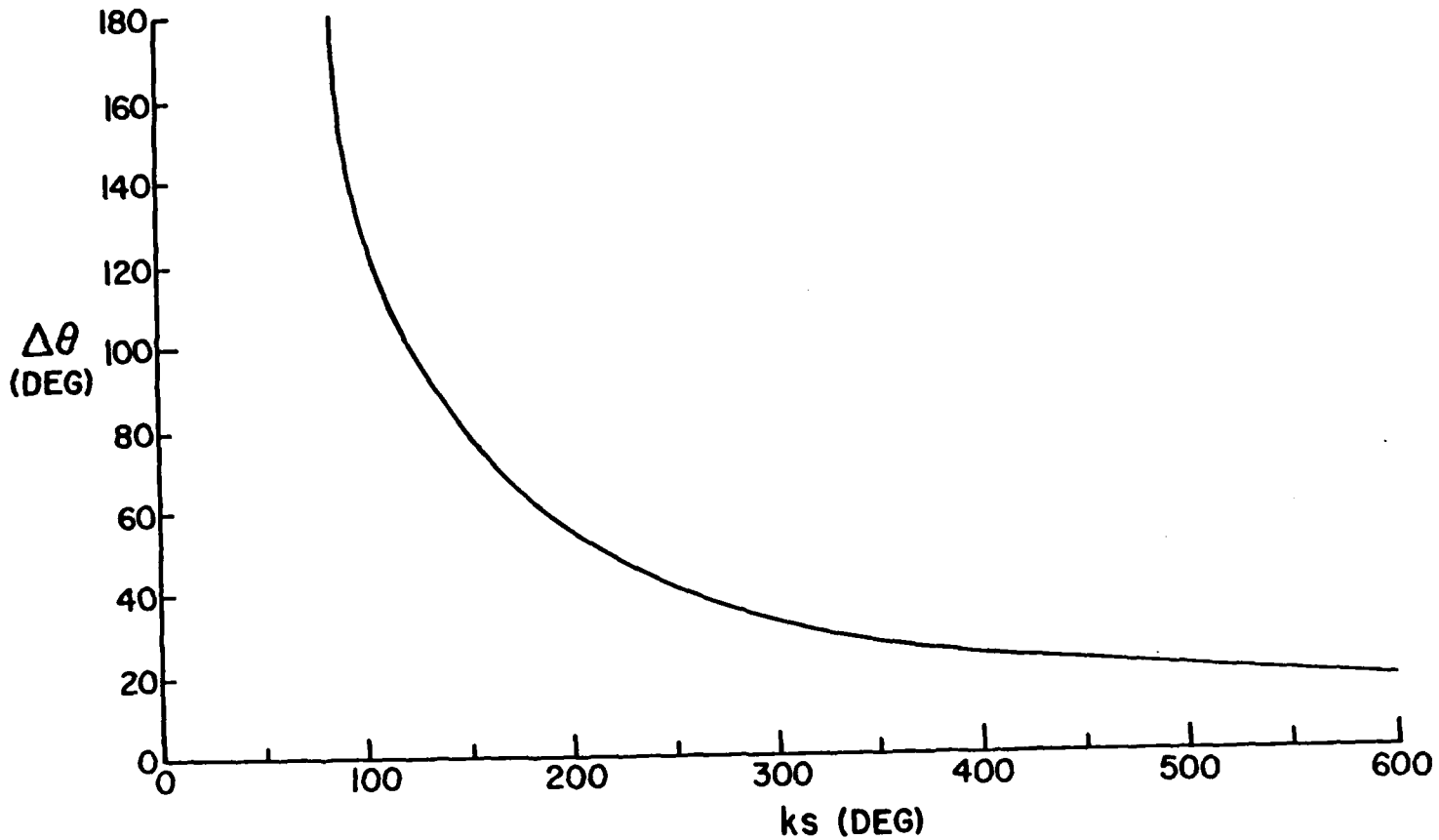

Figure 3.14

Array Beamwidth (3 dB) Versus Spacing

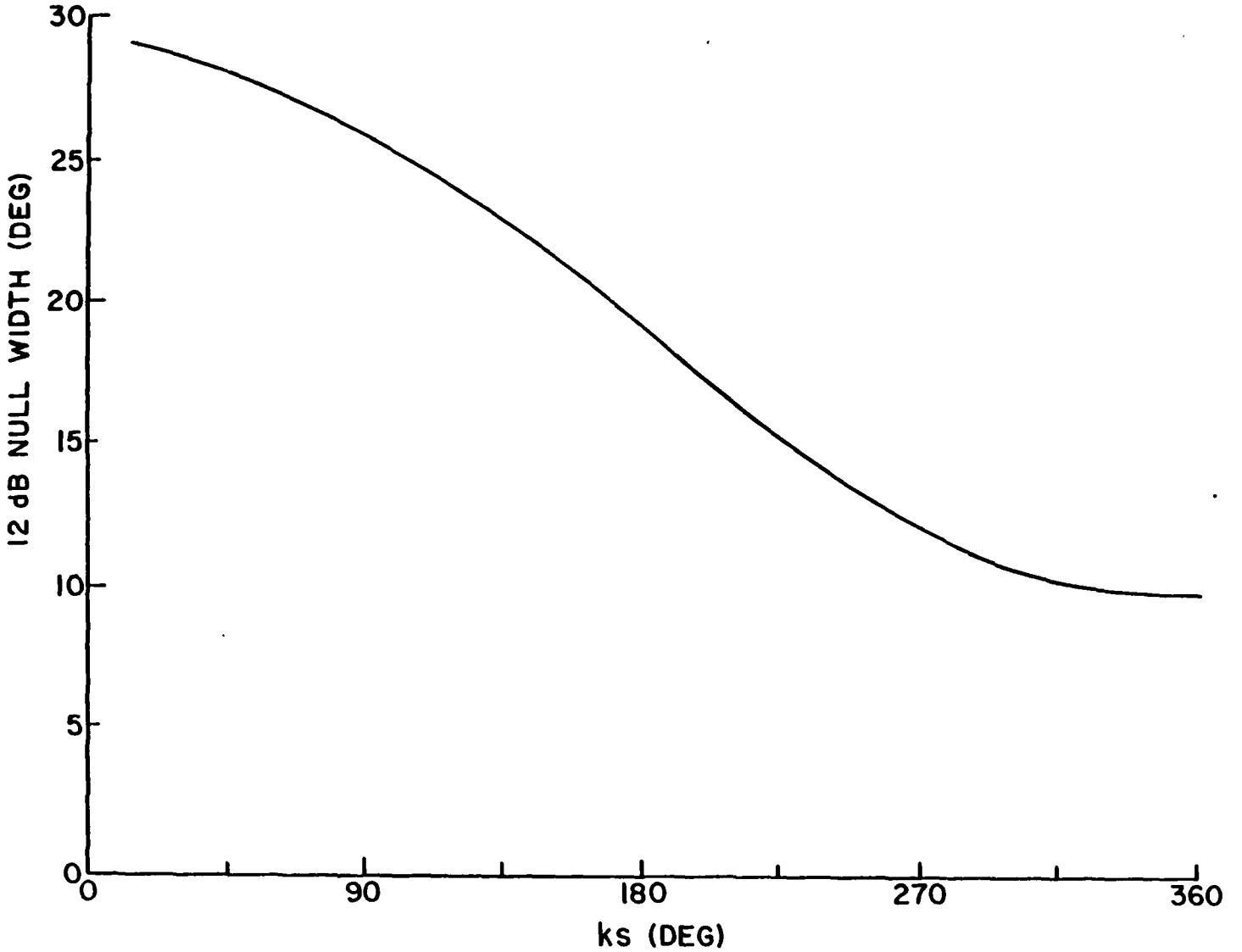

Figure 3.15

Array Null Width Versus Spacing

4. THE ARRAY SYSTEM

Figure 4.1 is a block diagram of the electronics which formed the array system. At the left is the instrumentation of the "Watson-Watt" direction finder. The Spears antenna is, in fact, two orthogonal loops complete with amplifiers; the outputs of which, after balancing and bandpassing, are introduced to the horizontal and vertical axes of an oscilloscope. The relationship between the loops and the cathode ray tube deflection plates is such that when an electromagnetic signal arrives from the north or south, the display is deflected vertically by an amount proportional to the amplitude of the signal. If the radiation arrives from the east or west, the deflection is horizontal; if from the northeast or southwest, the deflection is tilted at 45 degrees, etc. Because loop antennas have two maxima, 180 degrees apart, the system cannot tell the difference and displays both. The inclusion of a whip antenna and associated receiving electronics driving the z axis (intensity) eliminates the 180° ambiguity by blanking the screen when it would otherwise be writing the erroneous data. Ideally, the deflections should be straight radial lines, but a number of factors cause them to loop. One is the presence of a TE component of the sferics, slightly out of phase with the TM component. Another is an overlap of two or more pulses. Although not common with large sferics, this second effect becomes large as the noise under study gets small, soon rendering the display useless. Also, unless extreme care is taken to insure identical filtering, any slight phase shift between the x and y channels will cause loops to appear as the bandwidth is narrowed. For this study, the displays presented were of sferics noise at its peak frequency between 10 and 15 kHz, not at the operating frequency.

The measurement of an improvement in signal-to-noise ratio by the array requires a reference channel against which the antenna under test can be compared.

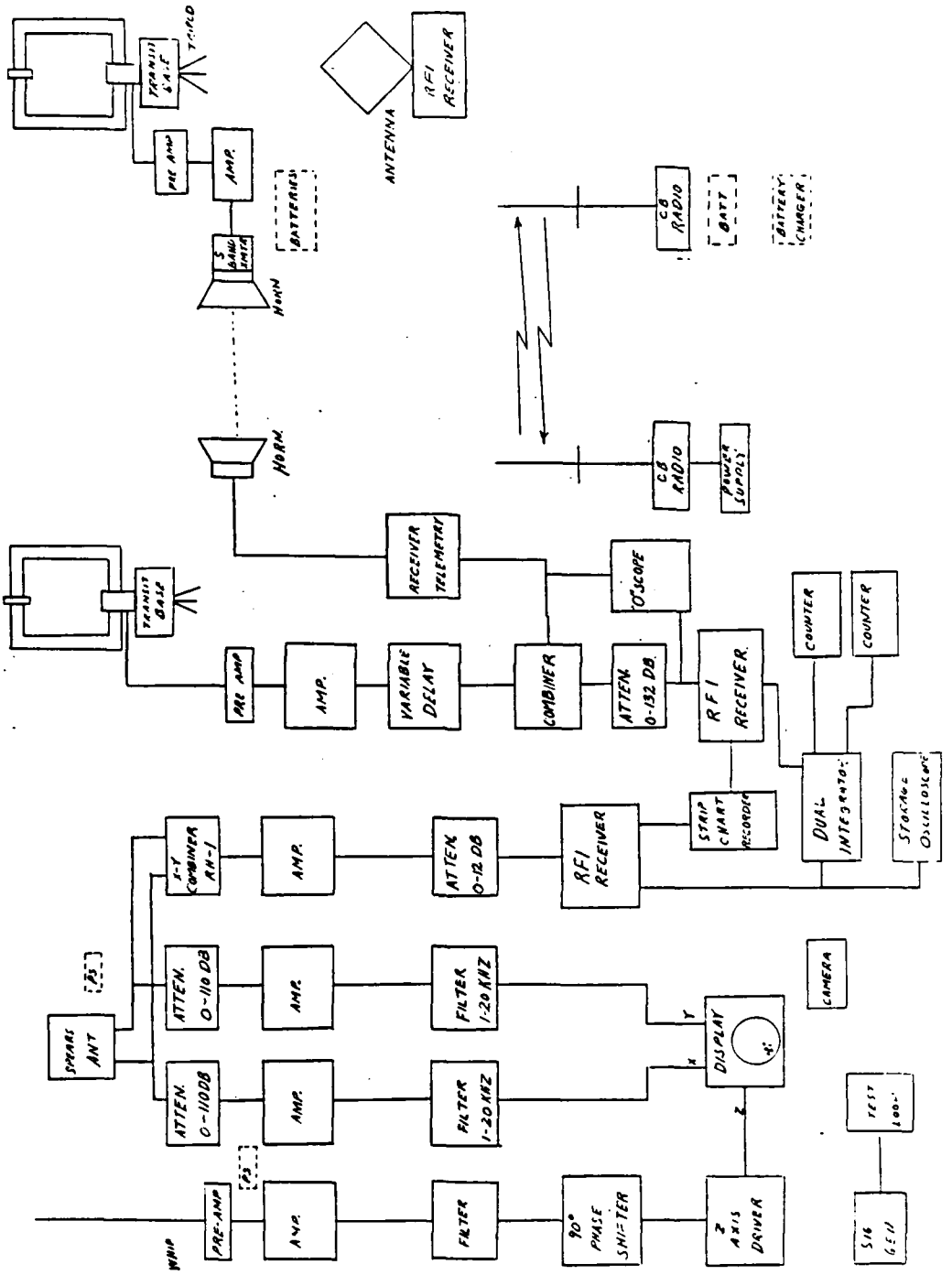

Figure 4.1 Block Diagram of the Phased Array System

It was decided that the reference antenna be omnidirectional in the horizontal plane, which was easily accomplished by properly combining the outputs of the two Spears loops. This signal was narrow band filtered (generally 100 Hz) with an RFI receiver nearly identical to that used for the array. The linear intermediate frequency output from this receiver was detected and integrated. As any electric circuit must have amplitude limits, the integrator was made to reverse at positive and negative thresholds, so that it would output a triangular wave when fed a steady signal. A standard counter counted and displayed the number of integrator reversals in a time determined by the operator's wristwatch, and then the average signal level could be computed.

Shown to the right in Figure 4.1 is the slave station. A receiving loop, about one meter square and resonant at about 100 kHz, was mounted on a rotatable transit base which, in turn, was mounted on a tripod. After amplification, its output modulated an S-band transmitter which broadcasted through a horn to a receiving horn located at the master station. The telemetry signal was demodulated with a receiver and fed to the combiner, where it was added to a signal received with essentially identical equipment less the telemetry apparatus and plus the steering delay line. The combined signal was inputted to a receiver whose I.F. output was detected, integrated, and counted just as was the reference signal. A comparison of these two counters provided the performance of the array relative to an omnidirectional antenna.

When a visual sighting allowed, the loops were geographically aligned by aiming them on landmarks taken from a map. When the horizon was obscured by trees, a magnetic compass was used. In both cases, double and sometimes triple checks were made by electrically nulling the antenna on some known radio source at some known great circle azimuth. Array separation and baseline direction were taken from maps.

The system portion of the telemetry delay was measured by erecting the two loops at the same place, parallel but opposed, and tuning the receiver to a known transmitter. Sufficient delay was injected to achieve the best null. The travel time portion of the telemetry delay was computed and the sum of these two, dubbed the "teledelay", was the base delay of the system. Its insertion in the master channel put the maxima of the antenna pattern perpendicular to the baseline.

Known transmitters were also used to balance the gains of the two array channels. After computing the delay necessary to steer the null toward a transmitter and injecting that delay, the gains of the two channels were adjusted for the best null achievable, and locked. Often no known transmitter existed at the operating frequency, and the system was balanced on two stations with frequencies bracketing the operating one, and a compromise drawn. The inability to calibrate and test at the operating frequency was a weakness of the experiment, but the installation of a sufficiently remote transmitter would have been a large undertaking.

After setting up, aligning, and balancing the system in preparation for a test, long (minutes) photographic exposures were made of the Watson-Watt display. These photographs provided a record of the intensity and azimuth of the storm activity. Figure 4.2 is a melange of such records, taken on different dates and times. In some cases the z-axis blanking channel was not connected. In others, it was rendered ineffective by an increase of gain well above design to allow examination of smaller sferics. Since the tests were performed in the early Spring in New England, it was believed that no storms were to the north, and the northerly indications were ignored.

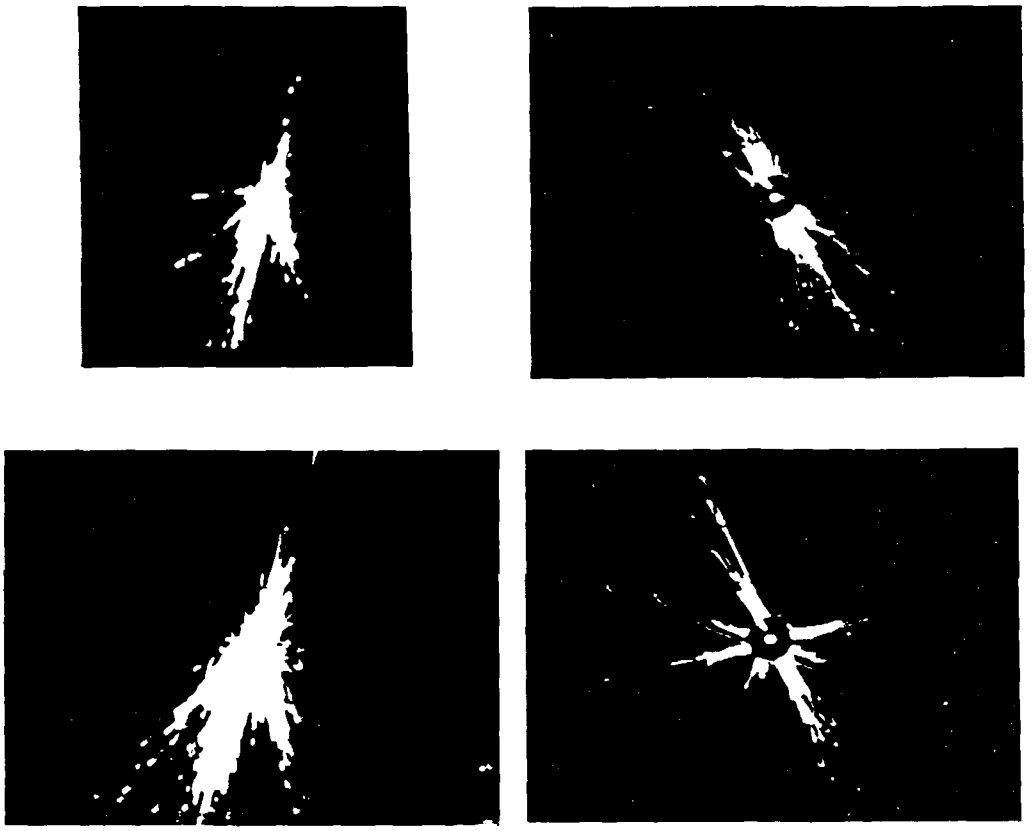

Figure 4.2 Watson-Watt Displays

The photographs were then compared with precomputed antenna patterns and the known direction of the desired source; and, with educated guessing, a delay and loop angle were chosen. The system was set to these parameters and the integrators started. After one or more minutes of integration, the counters were read and recorded, and the process restarted. On those few occasions when the source was inactive, similar measurements of the noise alone in both the array and reference channels were measured. Alternatively, the receivers were tuned away a few kilohertz, and noise measurements made. From this data the performance of the array was measured by computing the improvement in signal-to-noise ratio of its output and comparing to that of the omnidirectional antenna.

$$\frac{(s/n)_a}{(s/n)_r} = \frac{s_a/n_a}{s_r/n_r} \approx \frac{(s+n)_a/n_a}{(s+n)_r/n_r} \qquad 4.1$$

where s is a signal level, n is the noise level, the subscript a indicates the array and subscript r indicates the reference omnidirectional antenna. The approximation is within 10% for s/n values greater than 2.

5. THE FIELD PROGRAM

After initial assembly, the master station was reconstructed in Stow, MA at the Air Force Weather Station on the Fort Devens Annex. The slave station was located on Pinnacle Hill in Harvard, MA, 11.75 km away, bearing 330.5°T. Although both sites have towers extending above the surrounding trees, the distance, and the intrusion of a hill well into the first Fresnel zone rendered the telemetry link marginal. Intersite communication using citizen band radio was unsatisfactory. A computer was used to calculate and draw 121 antenna patterns for this separation and 35 kHz (ks = 493.5°), and 11 values each of ϕ and ζ. These were posted in a large mosaic, a reduced portion of which is shown in Figure 5.1. The intent was to provide a complete and easily used display to be compared with the noise distribution and from which the array steering parameters could be drawn. As can be seen, the pattern gets quite complex, with as many as eight nulls. Although only two of these are independent, the array provides a great deal of flexibility for the process of selecting the pattern of optimal noise reduction.

After a winter recess, the slave site was moved to an apple orchard on Gospel Hill in Hudson, MA. The separation was now 4.1 km and the baseline bearing 243.5°T. The teledelay was 17.9 usecs, and ks = 162.94° at a frequency of 31 kHz. The array pattern alone (removing the loop pattern terms) was calculated for incremements of 10° of the delay angle. Some of these are shown in Figure 5.2. The normalization has also been removed from the equations to aid in the use of these graphs as tools.

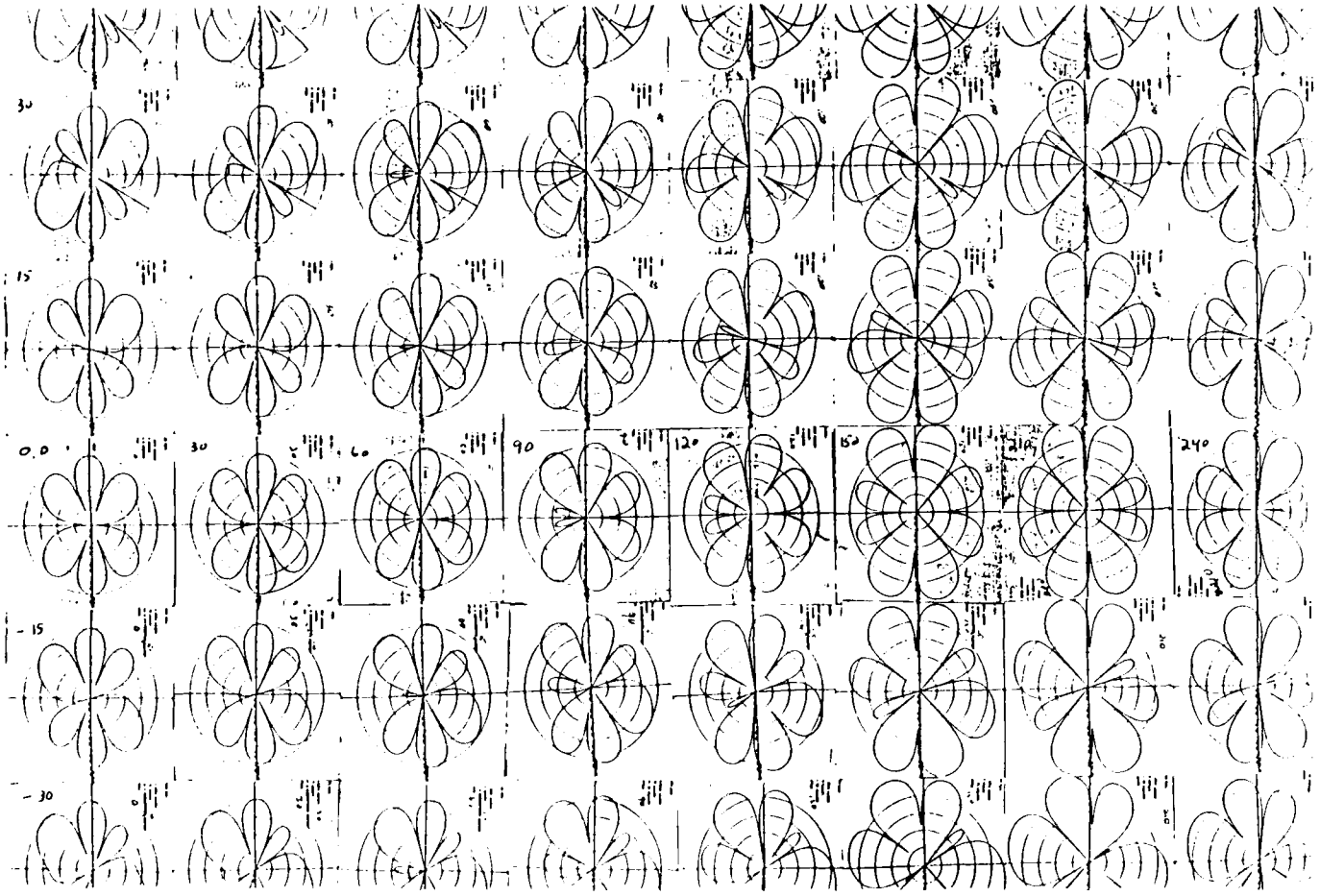

Figure 5.1 Mosaic of Array Patterns (ka=493.4)

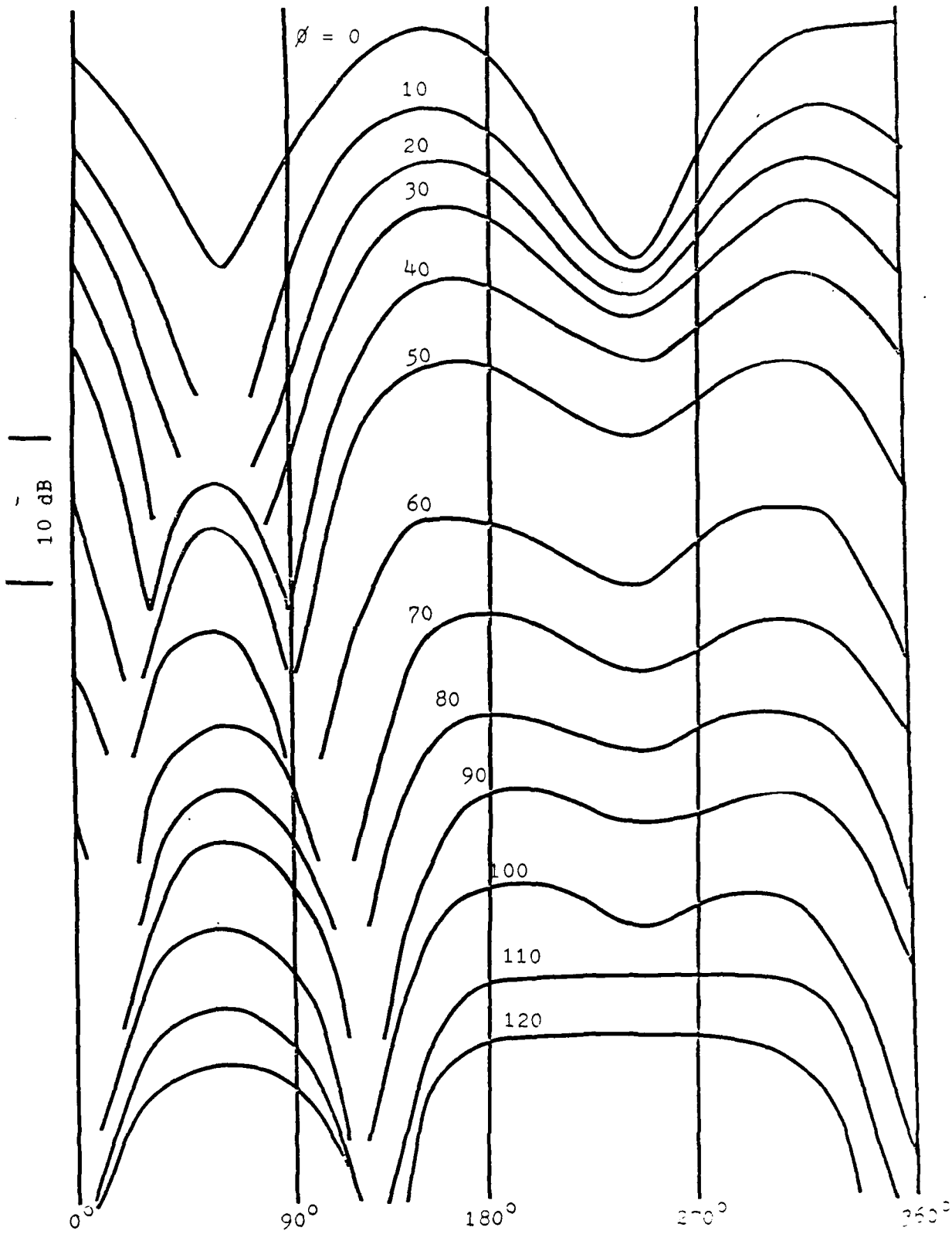

Figure 5.2 Array Patterns (no element, ks = 162.9)

The cosine pattern of the loops was drawn to the same scale on clear plastic and, in operation, was laid over the graphed array pattern selected. The logarithmic verticals were then eyeball added, creating the complete pattern. The overlay was slid from side to side on a number of array patterns before the parameters to be used were selected.

After having had some practice with noise alone, with stationary sources, and with transmitting aircraft, the capabilities of the array were demonstrated on 29 April 1983. On that afternoon an aircraft towing a long antenna flew in a racetrack pattern off the Virginia coast. The specifics of the flight are listed in Table 5.1. The Watson-Watt display photographs taken at various times are shown in Figure 5.3. Figure 5.4(a) through (e) shows the five antenna patterns used (incorporating the pattern of the loops). The short vertical lines drawn near the bottom of each pattern show the position of storms as indicated by the photos.

At about 1925UT the array was adjusted to produce the pattern shown in Figure 5.3(a). Measurements of signal plus noise and noise alone were made with both the reference antenna and the array. Improvements of 11 dB, 6 dB, and 4.7 dB were measured, the improvement decreasing as time progressed. At about 2025UT the array was changed to produce the pattern shown in Figure 5.3 (b). The aircraft was still heading almost directly at the array, and still modulating with a spread spectrum which had a wider bandwidth than the 100 Hz bandwidth of the array receiver. In the Figures the azimuth of the aircraft is indicated by a long vertical line. Measurements taken over the next half hour yielded array improvements of 7.1 dB and 11.7 db, in spite of the fact that there were storms directly along the transmitter azimuth.

TABLE 5.1. FLIGHT DATA FOR 29 APRIL 1983 CINCLANT TWA TRANSMISSIONS

True Air Speed (TAS)	-	410 kts
Altitude	-	32,000 ft
Wire Length	-	15,030 ft
Transmitted Power Measurements		
Mode 15	-	20 kW/ 90W reflected
Mode 9	-	20 kW/200W reflected

Mode 15 Transmissions (FSK)

Time	MSG	Heading	Start Time Geog. Coords
1907-1909	MSG X3	270	36.06N, 73.42W
1953-1955	MSG X3	010	35.42N, 73.35W
2039-2042	MSG X3	010	35.48N, 73.35W

Mode 9 Transmissions (Spread Sprectrum)

1912-1916	MSG	188	NA
1916-1933	MSG	240	NA
1958-2033	MSG	010 (w/turns)	NA
2045-2107	MSG	270 (w/turns)	NA
2107-2123	MSG	010 (w/turns)	NA

a. 1400

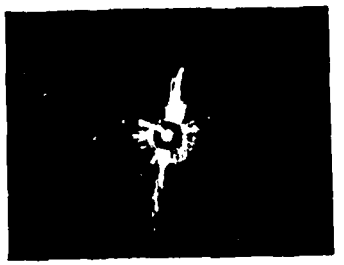

b. 1500

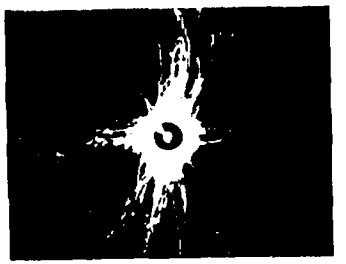

c. 1507

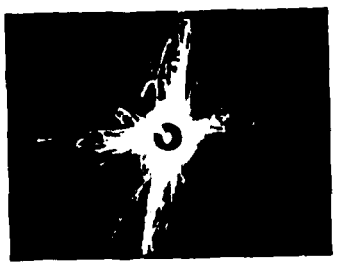

d. 1525

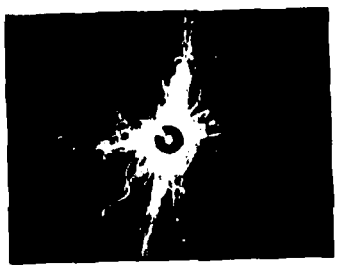

e. 1550

f. 1618

g. 1631

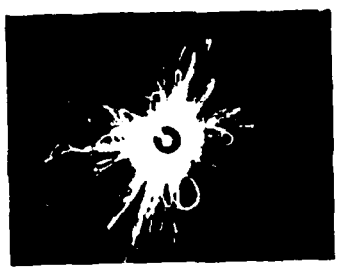

h. 1700

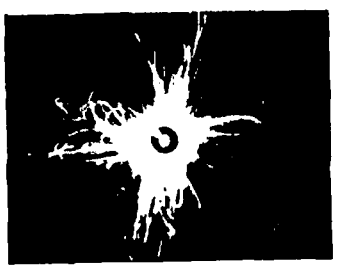

i. 1725

Figure 5.3 Watson-Watt Displays of Radiation from Electrical Storms, 29 Apr 83

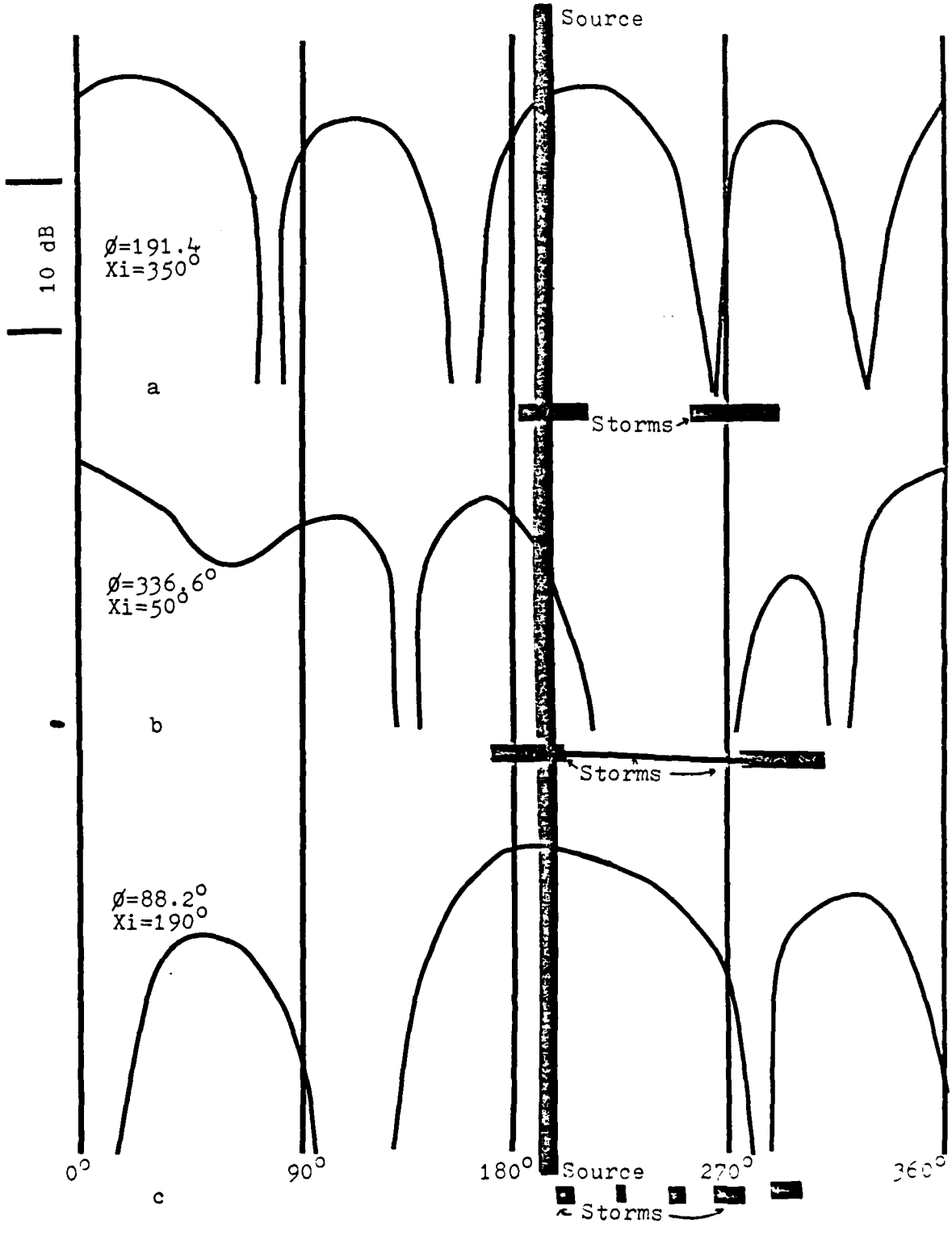

Figure 5.4 29 April Antenna Patterns

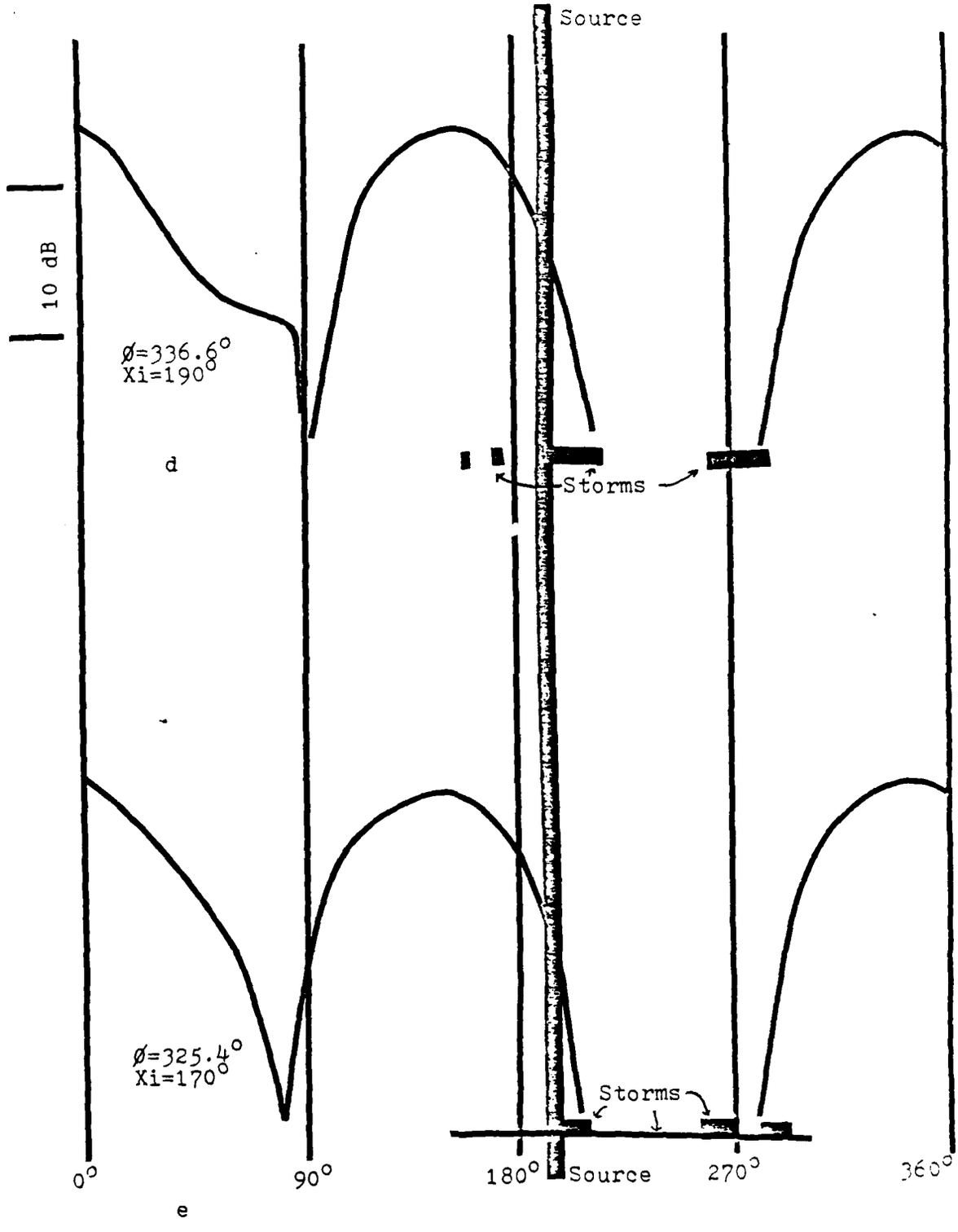

Figure 5.4 29 April Antenna Patterns

At 2055UT, the array pattern was adjusted to that shown in Figure 5.3 (c) and five measurements of signal plus noise were made (standard deviation of less than 6%) yielding an improvement of 12.8 dB. Slightly later an improvement of 10.6 dB was measured. The delay, but not the loop direction, was changed at 2105UT to that shown in Figure 5.3 (d) just as the aircraft turned to the west and presented the array a broadside view of its antenna. An improvement of 5.1 dB was measured. Again, at 2116UT the pattern was changed to that shown in Figure 5.3(e), and an improvement of 5.6 dB was measured.

6. CONCLUSIONS AND RECOMMENDATIONS

In spite of a noise situation far from ideal for displaying signal-to-noise improvement, with storms spread over large azimuthal angles instead of narrow angular bands, and with a storm directly behind the signal source, the demonstration regularly showed improvements of over 5 dB and as great as 12.8 dB. This could be equivalent to increasing transmitter power from 20 kW to 380 kW. Weaknesses in the array as constructed and operated became apparent during the tests. There was no way to accurately tune the system at the operating frequency. The process of reading the storm direction from a display of a few large sferics at a different frequency and then guessing the best array pattern needs improvement. It is not known with certainty that the azimuth of sferics measured at their peak frequencies near 12 kHz and the azimuth of the higher frequencies of interest were one and the same. Also, it is not known if the direction distribution of the large sferics displayed by the direction finder is the same as that of the average noise power which possibly may be heavily influenced by a preponderance of small sferics from large distances. Ideally, the azimuthal distribution of all the noise power should be measured at the operating frequency and the array parameters for maximum signal-to-noise ratio automatically computed.

It was originally proposed that more than two loops be incorporated into the array, thus producing more independently steerable nulls. It was also proposed that the array be converted to, and tried with, transverse electric radiation from the aircraft towing a long wire antenna. Investigation of these possibilities was not within the scope of the present work.

The performance of the array could be greatly improved by using the array itself to determine the directions of the noise sources rather than a different system operating at different frequencies, times, and amplitudes. Each station of the array should be equipped with two orthogonal loops and perhaps a monopole. An array control system would automatically determine and adjust the parameters necessary to steer the array and the elements for maximum signal to noise ratio. Such a system would produce signal to noise improvements significantly better than those demonstrated in these tests.

APPENDIX A

TWO THEOREMS ON NOISE MEASUREMENT WITH A ROTATING LOOP ANTENNA

Suppose the noise intensity is purely TM-polarized and distributed around the horizon as described by the function $N(\alpha)$, see Figure 1. Evidently $N(\alpha)$ is a periodic function with period 2π radians. Suppose, also, that the receiving antenna is a vertical loop, whose orientation is described by the angle θ, and whose amplitude response is a sinusoidal "figure of eight." With the loop set at angle θ', the noise power will be

$$P(\theta) = K \int_0^{2\pi} N(\alpha) \cos^2(\alpha-\theta) d\alpha \tag{1}$$

where K is a constant depending on the details of the equipment. Using standard trigonometric formulas,

$$P(\theta) = \frac{K}{2} \int_0^{2\pi} N(\alpha) \cdot [1 - \cos(2\alpha-2\theta)] d\alpha \tag{2}$$

$$= \frac{K}{2} \int_0^{2\pi} N(\alpha) d\alpha - \frac{K}{2} \int_0^{2\pi} N(\alpha) \cdot \cos(2\alpha.2\theta) d\alpha \tag{3}$$

$$= \frac{K}{2} \int_0^{2\pi} N(\alpha) d\alpha - \frac{K}{2} \cos 2\theta \cdot \int_0^{2\pi} N(\alpha) \cos 2\alpha d\alpha \tag{4}$$

$$- \frac{K}{2} \sin 2\theta \int_0^{2\pi} N(\alpha) \sin 2\alpha d\alpha$$

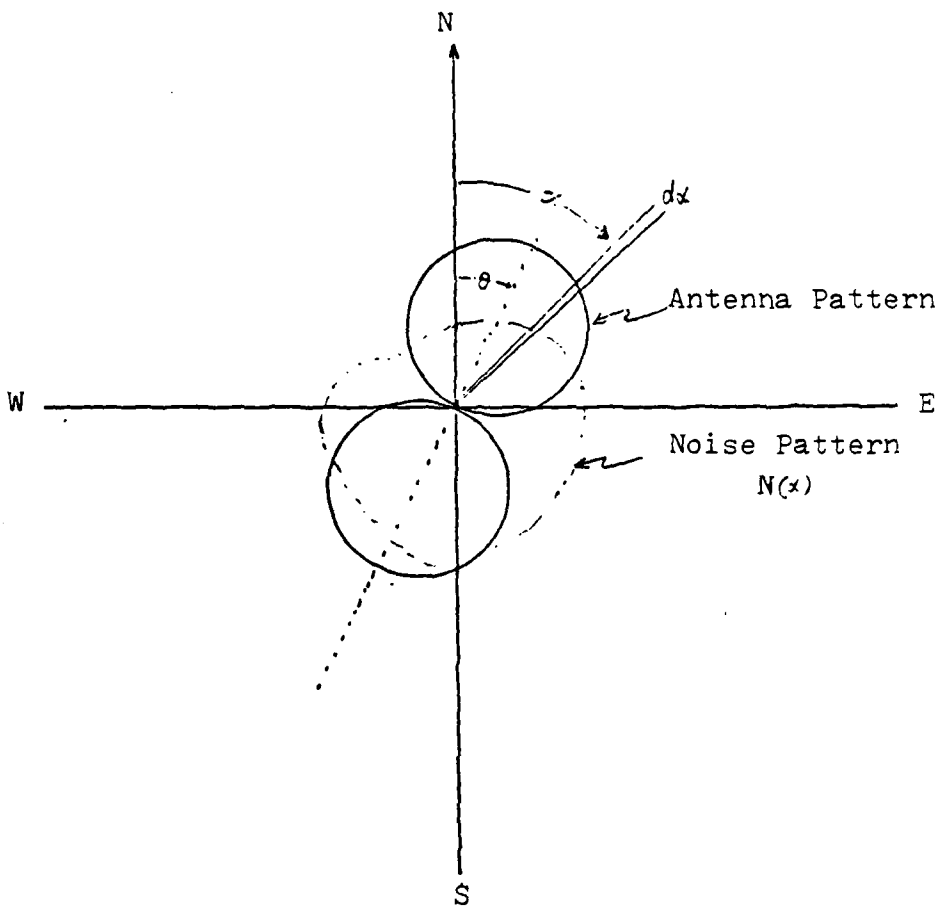

Figure A.1 Illustration of Noise and Antenna Patterns

Since $N(\alpha)$ has a period of 2π radians, it may be expanded in a Fourier series:

$$N(\alpha) = \frac{a_o}{2} + a_1 \cos \alpha + a_2 \cos 2\alpha + a_3 \cos 3\alpha + \ldots$$

$$+ b_1 \sin \alpha + b_2 \sin 2\alpha + b_3 \sin 3\alpha + \ldots \quad (5)$$

where for instance

$$a_o = \frac{1}{\pi} \int_o^{2\pi} N(\alpha) d\alpha \quad (6)$$

$$a_2 = \frac{1}{\pi} \int_o^{2\pi} N(\alpha) \cos 2\alpha \, d\alpha \quad (7)$$

$$b_2 = \frac{1}{\pi} \int_o^{2\pi} N(\alpha) \sin 2\alpha \, d\alpha \quad (8)$$

Then

$$P(\theta) = \frac{\pi K}{2} \left[a_o - a_2 \cos 2\theta - b_2 \sin 2\theta \right] \quad (9)$$

This may be rewritten in the form

$$P(\theta) = \frac{\pi K a_o}{2} \left[1 - Q \cos(2\theta - \phi) \right] \quad (10)$$

where

$$\phi = \tan^{-1} \frac{b_2}{a_2} \tag{11}$$

and

$$Q = \sqrt{\frac{a_2^2 + b_2^2}{a_o^2}} \tag{12}$$

Evidently, from inspection of Equations (6), (7) and (8),

$$a_2^2 \leq a_o^2 \tag{13}$$

and

$$b_2^2 \leq a_o^2 \quad , \tag{14}$$

so that Q is a positive quantity less than or equal to one.

The following theorems can now be stated.

THEOREM 1: No matter how complicated the noise distribution $N(\alpha)$ is, the the resulting noise curve distribution consists of a constant level upon which is superimposed a sinusoidal modulation with a minimum value at $\theta = \phi/2$ and a maximum value at $\phi/2 + \pi/2$.

THEOREM 2: Information about $N(\alpha)$ obtainable from $P(\theta)$ is limited to the Fourier coefficients a_o, a_2, b_2.

(a_o may be found directly, while a_2 and b_2 may be found from ϕ and Q.)

MISSION
of
Rome Air Development Center

RADC plans and executes research, development, test and selected acquisition programs in support of Command, Control Communications and Intelligence (C^3I) activities. Technical and engineering support within areas of technical competence is provided to ESD Program Offices (POs) and other ESD elements. The principal technical mission areas are communications, electromagnetic guidance and control, surveillance of ground and aerospace objects, intelligence data collection and handling, information system technology, ionospheric propagation, solid state sciences, microwave physics and electronic reliability, maintainability and compatibility.

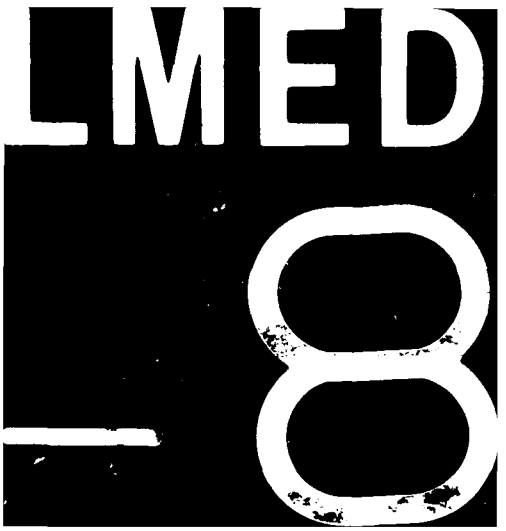
LMED
8